Regional carbon fluxes from an observationally constrained dynamic ecosystem model: Impacts of disturbance, CO_2 fertilization, and heterogeneous land cover

Ankur R. Desai,[1,2] Paul R. Moorcroft,[3] Paul V. Bolstad,[4] and Kenneth J. Davis[5]

Received 12 July 2006; revised 23 October 2006; accepted 2 November 2006; published 21 February 2007.

[1] The Ecosystem Demography (ED) model was parameterized with ecological, forest inventory, and historical land use observations in an intensively managed, wetland-rich forested landscape in the upper midwest United States. Model results were evaluated against a regional network of eddy covariance flux towers and analyzed about the roles of disturbance, forest management, and CO_2 fertilization. The model captured modern regional vegetation structure with worst comparison in wetlands. Model net ecosystem exchange of CO_2 (NEE) was highly correlated on monthly ($r^2 = 0.65$) and annual ($r^2 = 0.53$) timescales to 7 years of NEE observed at a 396-m-tall eddy covariance (EC) tower and to 2 years of growing season NEE from 13 regional stand-scale EC sites of varying cover and age ($r^2 = 0.64$). Model summer NEE had higher than observed net uptake for the tall tower and mature hardwood sites, and correlation to growing season ecosystem respiration at these sites was poor ($r^2 = 0.09$). Exclusion of forestry led to overestimation of aboveground living plant biomass accumulation by 109% between two forest inventory cycles (1996–2004). On the long-term (200 years), forestry significantly altered ecosystem cover and age, and increased NEE by 32%. CO_2 fertilization over that time period increased NEE by 93% owing to a doubling of plant density. While the model showed that harvest and afforestation had smaller impacts on NEE than CO_2 increase, the former were still significant and require consideration when making future NEE predictions or scaling plot-level data to regional and global flux estimates.

Citation: Desai, A. R., P. R. Moorcroft, P. V. Bolstad, and K. J. Davis (2007), Regional carbon fluxes from an observationally constrained dynamic ecosystem model: Impacts of disturbance, CO_2 fertilization, and heterogeneous land cover, *J. Geophys. Res.*, *112*, G01017, doi:10.1029/2006JG000264.

1. Introduction

[2] It is difficult with direct scaling of eddy covariance flux tower measurements [e.g., *Desai et al.*, 2007] and coarse resolution biogeochemical models [e.g., *Heinsch et al.*, 2006] to adequately capture spatial gradients [*Ahl et al.*, 2004] or provide process understanding of regional land-atmosphere CO_2 flux. Models of ecosystem-atmosphere exchange offer the unifying framework needed to assimilate observations, extrapolate data points across space and time, and predict future change [*Moorcroft*, 2003]. Most coupled and uncoupled ecosystem-atmosphere models are driven primarily by net incoming radiation, meteorology and a "big-leaf" representation of regional average radiation and climate sensitive ecosystem parameters that vary with biome, mean climate, soil type, and elevation [*Moorcroft*, 2003]. However, spatial and temporal variability in ecosystem-atmosphere fluxes are functions of both exogenous, abiotic variability arising from variations in the physical landscape and climate, and endogenous, biotic variability driven by stochastic tree mortality and disturbance processes.

[3] Since biotic ecosystem dynamics (e.g., disturbance, mortality, reproduction) are typically more likely than abiotic variability (e.g., climate, soils, topography) to occur on small spatial scales, develop over long timescales, and have a stochastic component, they are often ignored, or modeled with simple, externally prescribed events [e.g., *Thornton et al.*, 2002]. These mortality and disturbance processes, along with prior anthropogenic modification of disturbance regimes, however, may lead to nonlinear feedbacks and leave an imprint on current ecosystem structure and fluxes [*Law et al.*, 2004; *Schimel et al.*, 1997].

[1] Institute for Integrative and Multidisciplinary Earth Studies (TIIMES), National Center for Atmospheric Research, Boulder, Colorado, USA.
[2] Formerly at Department of Meteorology, Pennsylvania State University, University Park, Pennsylvania, USA.
[3] Department of Organismic and Evolutionary Biology, Harvard University, Cambridge, Massachusetts, USA.
[4] Department of Forest Resources, University of Minnesota, Saint Paul, Minnesota, USA.
[5] Department of Meteorology, Pennsylvania State University, University Park, Pennsylvania, USA.

0148-0227/07/2006JG000264

[4] Mounting evidence from inventory estimates, ecosystem models, and atmospheric inversions suggests that ecosystem recovery from prior land clearing is responsible for a substantial portion of the modern observed North American carbon sink [*Caspersen et al.*, 2000; *Hurtt et al.*, 2002; *Pacala et al.*, 2001; *Schimel et al.*, 2001]. Several ecosystem models are able to incorporate prescribed disturbances [e.g., *Masek and Collatz*, 2006; *Thornton et al.*, 2002] and there is emerging application of global-scale coarse-resolution dynamic ecosystem models [e.g., *Cramer et al.*, 2001; *Foley et al.*, 1996]. However, explicit incorporation of processes leading to small-scale, stochastic disturbances has been, until recently, limited to gap-scale ($\sim$10 s of m) models. Computational ability prohibits use of gap models at the regional or global scale. An example of a new class of ecosystem models is the Ecosystem Demography (ED) model [*Moorcroft et al.*, 2001]. ED uses a statistical-dynamic approach to capture the mean impact of gap-scale subgrid disturbances on the model grid scale and regional scale, similar to other size-structured models [e.g., *Pacala and Deutschman*, 1997], but with specific incorporation of the net effect of stochastic disturbance events and prescribed harvest events on stand age distribution and development.

[5] Dynamic ecosystem models, however, are difficult to parameterize and evaluate. There is growing interest in using eddy covariance flux towers for both model evaluation [e.g., *Hanson et al.*, 2004] and parameter optimization [e.g., *Braswell et al.*, 2005; *Knorr and Kattge*, 2005; *Ricciuto et al.*, 2007; *Sacks et al.*, 2006]. However, careful selection of eddy covariance tower networks and ancillary data are required for dynamic ecosystem model assimilation or evaluation so as to ensure that the full range of ecosystem complexity relevant to carbon exchange is characterized.

[6] Forest inventory techniques provide a complementary method to quantify current biomass and flux across larger spatial scales [*Jenkins et al.*, 2001; *Smith et al.*, 2004]. While spatial sampling density of inventory methods is high, national inventory programs typically suffer from long (multiyear) measurement intervals, lack of observations in all carbon pools, and ecosystem sampling biases. Still, inventories can be used to derive disturbance, mortality, and ecosystem structure parameters for ecosystem models.

[7] We applied the ED model at the regional scale to test the influence of disturbance and land cover variability on ecosystem structure and CO_2 fluxes. Forest inventory biomass, density, mortality, land cover data, remotely sensed land cover, preinventory land use history data, and ecophysiological field observations were used to initialize and parameterize the model. Input variables of historical meteorological observations and atmospheric CO_2 proxies were used along with automated, tower-based hourly observations of these variables made since 1996.

[8] The region of study is north-central Wisconsin in the upper midwest, United States, location of the Chequamegon-Ecosystem Atmosphere Study (ChEAS: http://cheas.psu.edu). A unique aspect of ChEAS is the globally unique eddy covariance flux measurements made since 1995 on a very tall (447 m) television transmitter (WLEF) near Park Falls, Wisconsin. Over the years, as many as 11 other stand-scale flux towers were in operation in the region across a range of 14 vegetation and stand age categories [*Desai et al.*, 2007]. The very tall tower has observed a small annual source of CO_2 to the atmosphere since the measurement campaign started [*Davis et al.*, 2003; *Ricciuto et al.*, 2007]. In contrast, most of the stand-scale towers observed sinks of CO_2 [*Desai et al.*, 2007]. An ecosystem model that did not include disturbance or land-use overestimated daytime growing season net CO_2 uptake compared to the tall tower [*Baker et al.*, 2003]. Prior stand-scale flux tower upscaling [*Desai et al.*, 2007] and tall tower downscaling [*Wang et al.*, 2006] suggested that forested wetlands and recently disturbed forests are undersampled and potentially explained the CO_2 source observed by the tall tower flux measurement.

[9] The parameterized ED model provides an alternative, independent estimate of regional flux, based entirely on an integration of forest inventory, historical meteorology and ecological data. Fluxes measured from the tall tower and the multitower upscaling allowed for evaluation of ED model performance. The ED model was then used to test the hypothesis that the impact of disturbance in the footprint of the tall tower on net CO_2 flux was underestimated by the stand-scale towers. The parameterized model was also used to test whether or not land use history and CO_2 fertilization over the past 150 years had a significant impact on the current forest structure and CO_2 fluxes in the region.

2. Methods

2.1. Site Description

[10] Observational data were collected and the model was parameterized over north-central Wisconsin, located in the upper midwest region of the United States, in an area centered on the Park Falls, Wisconsin WLEF eddy covariance tower. The region is heavily forested, lacks sharp elevation gradients and has a low human population density. The primary forest types include mature northern upland mesic hardwoods (*Acer spp.*, *Tilia americana*, *Betula alleghaniensis*, *Fraxinus spp.*) and younger aspen (*Populus termulouides*), with smaller coverage of xeric softwoods and hardwoods such as red pine (*Pinus resinosa*), balsam fir (*Abies balsamea*), and jack pine (*Pinus banksiana*) [*Desai et al.*, 2007]. Forested and shrub wetlands and grassy meadows cover close to 30% of the region, typical of glacial outwash landscapes in this region. Primary wetland trees include black spruce (*Picea mariana*), white cedar (*Thuja occidentalis*), tamarack (*Larix laricina*), alder (*Alnus spp.*), and willow (*Salix spp.*) species [*Desai et al.*, 2007].

[11] Forests, both public and private, are heavily managed, though the magnitude of forest harvest is in decline [*Frelich and Reich*, 1995]. The region was heavily clear-cut from the mid-nineteenth to early twentieth century. Presettlement upland forest consisted primarily of upland eastern hemlock (*Tsuga canadensis*), northern hardwoods and white pine (*Pinus strobus*) [*Schulte et al.*, 2002]. Natural disturbance is dominated by extreme meteorological or climate events (e.g., wind storms, drought), while large-scale fire is rare [*Frelich and Reich*, 1995]. Given the large diversity in vegetation cover type and age but minimal variation in climate across space, the region allows for investigation of the role of biotic factors and anthropogenic disturbance on

ecosystem-atmosphere flux and forest structure while minimizing the effect of climatic gradients.

2.2. Ecosystem Demography Model

[12] Forest gap models are dynamic ecosystem models that track the fate of every plant and associated biogeochemical flux within the scale of a single overstory canopy tree [*Pacala et al.*, 1996]. The model is called a "gap" model since it is the stochastic dynamics of disturbance in canopy individuals that leads to dynamic ecosystem evolution via release and growth of subcanopy species in canopy gaps. Using these gap models at scales larger than a forest stand is limited both by computational ability and stochastic instability/sensitivity to initial conditions. Instead, *Moorcroft et al.* [2001] argue that for scales with sufficiently large numbers of gaps, regional biogeochemical cycling and ecosystem structure can be captured by modeling the time evolution of an ensemble average of all gaps, similar to the statistical-mechanical approach used in modeling turbulent fluid transport as parcels of fluids instead of tracking the fate of every molecule.

[13] The key to a well-formed ensemble average is conditioning the ensemble with respect to the key differences among gaps that lead to heterogeneity in ecosystem structure across space. *Moocroft et al.* [2001] showed that a plant cohort size– and gap age–structured mean-moment model explicitly conditioned on stand age since disturbance properly accounts for the primary resource variability leading to ecosystem structural differentiation and competition, namely heterogeneity in the subcanopy light environment as a function of stochastic disturbance of canopy trees. This insight forms the basis of the ED model. Partial differential rate of change equations (PDEs) for plant community evolution in size and plant functional type distribution as functions of growth, mortality, seedling recruitment, and disturbance rates are derived for ensemble-average gaps of different ages since disturbance (Appendix A).

[14] The original model was parameterized for use in South American tropical forests and grasslands [*Moorcroft et al.*, 2001]. *Hurtt et al.* [2002] extended the original model for use in North America, defining three new plant functional types (cold-deciduous trees, coniferous trees and C3 grass types), reparameterizing the probability of fire disturbance, and spread and extending the model to incorporate anthropogenic disturbance and land-use change. Land-use change was incorporated by specifying a land-use transition matrix to track the movement of land between different land-use classes. *Albani et al.* [2007] further refined the model for use in the northeastern United States parameterizing seven new plant functional types (early, mid, and late successional deciduous tree types, northern pines, southern pines, and late successional conifer trees) and adding a new disturbance routine for pathogen outbreaks. More recently, a coarse woody debris (CWD) submodel has been added (P. Moorcroft et al., unpublished paper, 2004) that tracks the fate of dead structural material into the structural soil carbon pool.

[15] To apply the model to this study, several other modifications were made. Individual grid cells in the model, typically $1^\circ \times 1^\circ$ in resolution, are considered independent in ED. The ED equations essentially describe the subgrid biotic dynamics assuming abiotic factors across the grid cell are constant. The focus of this study was to test the role of biotic dynamics in explaining regional flux since climate variability across the region was shown to be negligible [*Desai et al.*, 2007]. The model was recast as a single-region model consisting of essentially one 40-km-radius grid cell centered on the Park Falls, Wisconsin, tall tower. However, abiotic variation due to soil type and topography could not be neglected in the footprint, so the grid cell was divided into three independent models: mesic northern upland hardwoods, xeric conifer/mixed forests, and lowland forest/wetlands, with each having its own soil type, soil moisture retention, initial plant community, plant functional types, and forest harvest parameters. Minor changes were also made in the biogeochemical functions to better reflect plant dynamics in northern forests as detailed in the appendices.

2.3. Input Variables

[16] Primary time-varying forcing variables needed by ED are monthly air temperature (for respiration, phenology, and sapling mortality), minimum air temperature (for frost mortality), growing degree days (for phenology), number of days below 0°C (for phenology and snow hydrology), near-surface soil temperature (for soil decomposition turnover, plant water uptake and seedling germination), incoming precipitation (for canopy filtration and soil moisture), land-use transition rates, and forest harvest rates. Additionally, hourly midcanopy air temperature, surface-layer atmospheric CO_2 concentration, incoming photosynthetically active radiation (PAR), and vapor pressure deficit (VPD) are required for solving leaf-level assimilation and evaporation. All of these values were assembled from a combination of historical and current observed climate and forest resource data, as described below.

2.3.1. Meteorology and CO_2

[17] Daily quality-controlled temperature and precipitation data from National Climate Data Center archived weather station data of daily maximum and minimum temperature, total precipitation in Minocqua, Wisconsin (1905–1947), and Park Falls, Wisconsin (1948–2004), were provided by the U.S. Historical Climatology Network (HCN) [*Hughes et al.*, 1992]. Climate pre-1905 was assumed to repeat 1905–2005 values cyclically. The MT-CLIM algorithm was used to estimate daily total incident solar radiation and VPD from diurnal temperature range, precipitation, and time of year [*Bristow and Campbell*, 1984; *Kimball et al.*, 1997].

[18] The Park Falls, Wisconsin, tower provided hourly micrometeorological data from 1996–2004. These data were used to generate synthetic hourly data in the past using a random similarity matching algorithm. For each day without hourly data, meteorological fields were populated with a random member from a subset of days with hourly data that matched closest in mean daily temperature, diurnal temperature range, and solar radiation. If no days matched the criteria, then a 9-year diurnal average for the day was chosen, corrected for difference in diurnal temperature range. This synthetic hourly data were then used to generate the monthly climate variables required by ED.

[19] Carbon dioxide mixing ratios were derived from a combination of ice core CO_2 proxy measurements (prior to 1959) [*Robertson et al.*, 2001], the U.S. National Oceanic and Atmospheric Administration (NOAA) monthly atmo-

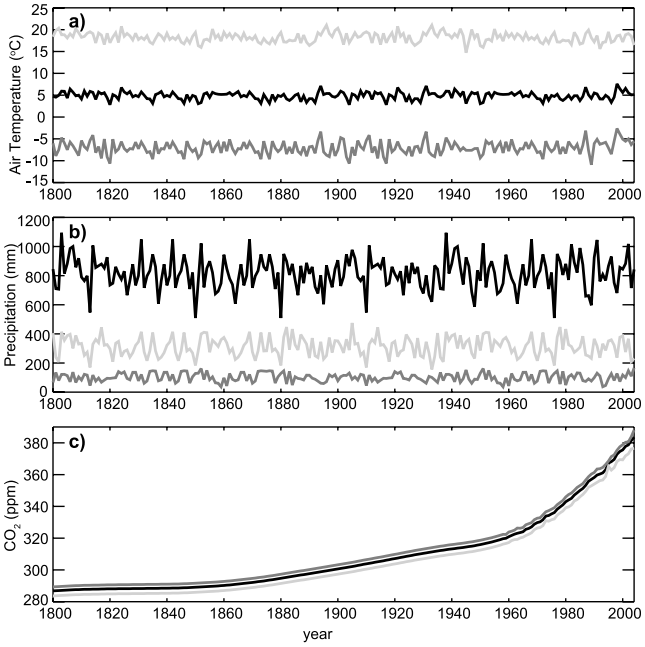

Figure 1. Annual (black line), summer (light gray line), and winter (dark gray line) (a) average air temperature, (b) total precipitation, and (c) atmospheric surface layer CO_2 concentration.

spheric CO_2 (1959–2004) [*Keeling and Whorf*, 2005], and hourly surface-layer CO_2 concentration at 30 m from the Park Falls, Wisconsin, tall tower (1995–2004) [*Bakwin et al.*, 1995]. A linear trend between annual mean CO_2 and annual 1-sigma variance in CO_2 was found from the Mauna Loa record and applied to the proxy CO_2 to create monthly CO_2 pre-1959. CO_2 concentration offsets between the long-term records and the tall tower were applied to create a synthetic continental CO_2 monthly data set. Monthly ensembles of diurnal CO_2 as fraction of monthly mean CO_2 were derived from the tall tower record and applied to the pre-1995 monthly CO_2 to create a consistent hourly CO_2 data set. Including diurnal and monthly CO_2 cycles in the biogeochemical model created a more realistic representation of the atmospheric environment experienced by a canopy leaf, though the overall impact of including these cycles in ED did not significantly affect ecosystem-atmosphere fluxes.

[20] Hourly meteorology was used to drive the leaf-level biogeochemistry in ED and allowed for inclusion of impacts of short-term weather and synoptic cycles on temperature, cloudiness and humidity. Growing-season modeled open stomata assimilation values were generally consistent with field observations of maximum leaf-level assimilation in an old-growth hardwood forest [*Kreller*, 2005]. However, preliminary comparisons suggested that transpiration values appeared to be high compared to scaled sap flux observations [*Tang et al.*, 2006].

[21] Hourly values were integrated to monthly forcing variables needed for vegetation dynamics modules. Monthly soil temperature was found by calculating the mean monthly difference in observed air and soil temperature in a mature forest averaged over several years and applying that to the entire air temperature record. Changes in the strength of soil temperature to air temperature differences were found from tower-based observations with higher and lower canopy leaf area, which were used to modify ED soil temperature algorithms to account for radiation penetration to the forest floor. Additionally, ED was modified so that a positive snow depth kept near-surface soil temperature at 0°C.

[22] Strong seasonality in climate was evident in the region as diagnosed by mean monthly temperature and precipitation climate input to ED from 1800–2004 (Figure 1). A long dormant season over the cold, dry winter is interjected by a short, mild, wetter summer. Annual variability in average seasonal temperatures was minimal, with winter variability exceeding summer. The growing season typically lasted mid-May to late September. Annual precipitation variability was driven mostly by variability in the growing season. Long-term trends over the twentieth century in temperature or precipitation are not evident, except for a recent trend of warmer winters.

2.3.2. Land Use and Forestry

[23] Decadal statistics on statewide forest harvest [*Adams et al.*, 2006] and historical forest land cover [*Birdsey and Lewis*, 2003] from U.S. Forest Service (USFS) reports and FIA and spatially gridded agricultural clearing and abandonment estimates from historical records [*Ramankutty and Foley*, 1999] were used to populate land use change transition matrices and harvest rate records. Remotely sensed and historical estimates of regional forest cover across Wisconsin were used to correct statewide data to regional averages. Decadal average values were linearly interpolated to annual values of forest cover which were then differenced to compute rates of forest gain and loss.

[24] Rates needed by ED are clearing of primary forest for agricultural use, clearing of secondary forest for agricultural use, abandonment of agricultural land to secondary forest, harvest of primary forest, and harvest of secondary forest. Pre-European settlement vegetation surveys [*Schulte et al.*, 2002] were used as initial state of vegetation cover in 1800. Historical analysis of loss of old-growth forest [*Frelich*, 1995] and modern land cover from FIA and remotely sensed estimates were used to constrain the forest gain/loss and agricultural clearing rates and convert them into the transition and harvest rates used in ED. To simplify the calculation, proportions of nonagricultural vegetated land that are mesic hardwood, xeric hardwood, and wetland were assumed to be constant over the period. No harvest was assumed to occur on wetlands. This method constrained ED land cover to be consistent with historical and current land cover.

[25] Land use transition and forest harvest rates (Figure 2a) and resulting land cover (Figure 2b) as derived from presettlement land cover and long-term harvest and agricultural land cover records revealed the dramatic impact of forest clearing. Rapid land clearing peaked in the mid-nineteenth century and removed most of the primary (successional end point) forest in the region by the end of the nineteenth century. Harvest of secondary (regrowth) forest peaked at the end of the nineteenth century and rapidly declined until 1950, with slower declines afterward. Clearing for agriculture or settlement occurred at a minimal rate over the period due to the limited suitability of the region for crops, with agricultural land cover peaking around 1950 and declining afterward. Consequently, woody encroach-

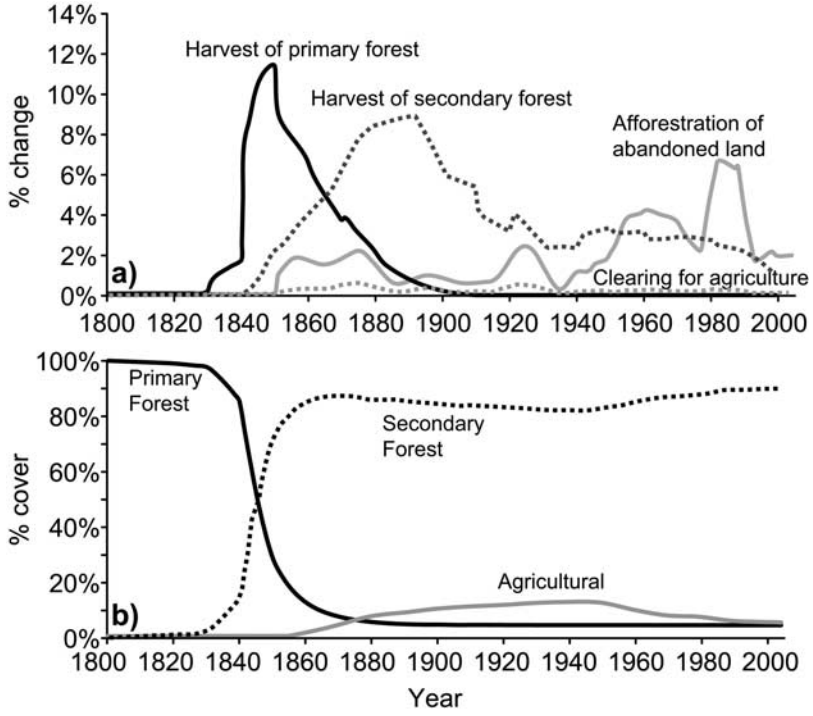

Figure 2. Annual (a) land use transition rates and (b) resulting land cover fraction of vegetated land by primary (black line), secondary (dotted line), and agricultural (gray line) gap disturbance origin for the model domain. The forest was essentially clear-cut in the late nineteenth century and a short-lived agricultural period diminished in the second half of the twentieth century.

ment in abandoned agricultural fields increased the amount of secondary forest. Land cover transition rates were generally consistent with a new nationally gridded land use transition database (G. Hurtt, personal communication, 2005).

[26] Modern observations of remotely sensed land cover type were used to apportion vegetated land into the three edaphic classes of forest (mesic upland = moist soil, mainly northern hardwood; xeric upland = dry soil, mainly conifers; lowland/wetland = forested and shrub wetlands), and the noninteracting agriculture and water land classes as used by ED (Figure 3). The primary assumption here is that the percent of vegetation fraction represented by each subregion was constant over time. Most likely this understates land cover variability and transition owing to draining of wetlands, variability in water table depth and change in soil cover and land use leading to wider planting of conifers. However, these rates were not available. Additionally, ED would require a more sophisticated 3-D hydrology module to handle moisture-disturbance interaction. Consequently, there is reason to believe the model understates total carbon fluxes owing to change in land use (e.g., pulse respiration at upland/wetland edges).

2.4. Model Setup

[27] As noted earlier, ED was run in the ChEAS region centered on the Park Falls, Wisconsin, tall tower with initial vegetation provided by pre-European witness tree land cover statistics [*Schulte et al.*, 2002]. Data on dominant and codominant species were used to parameterize ED initial land cover, under the assumption that all patches were old-growth in 1800. Species density was based on an uneven-age mixed species stand density index (SDI) formulation [*Woodall et al.*, 2005]. The SDI index formulation creates an exponentially declining statistical distribution of tree density per patch as a function of diameter at breast height (DBH, m) under the constraint of total basal area equal to the basal area of 24.5 m^2 ha^{-1} (i.e., 500 individuals ha^{-1} at 25 cm DBH). DBH range was calibrated against modern observed minima and maxima from FIA and field

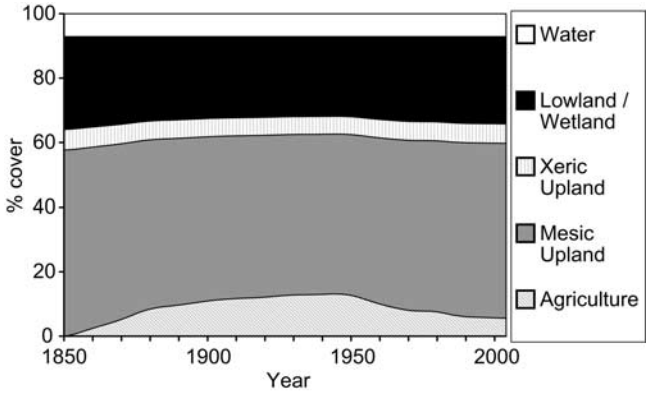

Figure 3. Annual assumed regional land cover fraction for water (white), lowland/wetland (black), xeric upland (lines), mesic upland (gray), and agriculture (slanted lines) based on historical land use transition rates conditioned on modern-day remotely sensed land cover. This land cover time series allows for modeling of the upland-wetland mosaic endemic in the region.

Table 1. ED Subregions and PFT Types Used in This Study

Abbreviation	PFT
Mesic Upland/N. Hardwoods	
GR	grass
AS	aspen
BI	birch
SM	sugar maple/basswood
HE	hemlock/spruce
Xeric Upland/Mixed Conifer	
GR	shrub/pine barren
JP	jack pine
RP	red pine
WP	white pine/fir
RM	red maple/oak/ash
Lowland/Wetland	
GR	meadow grass
AW	alder/willow shrub
TM	tamarack
CE	cedar
BS	black spruce

observations in old forests. SDI calibration was based on observations of stand density in an old-growth forest in the upper Peninsula of Michigan [*Desai et al.*, 2005].

[28] The primary abiotic gradient in the region (soil type-vegetation association), is described as previously noted with three submodels (Table 1), each with five plant functional types (PFTs). The long-run model was run from the start of settlement in 1800 until 2004. Shorter runs (1996–2004) were performed for parameter optimization using FIA observations in 1996 as the initial land cover.

[29] Model spinup for soil and water pools is fast (decades), so a long spinup run was not needed. Four scenarios were run on the 1800–2004 run to test the hypotheses on the role of past land-use change and carbon fertilization on modern ecosystem-atmosphere fluxes. These scenarios were (1) Full: all dynamics; (2) NO_CO_2: no anthropogenic-driven increase in CO_2 with time (repeat CO_2 concentration from 1800–1905 in 1905–2004); (3) NO_For: no forest harvest or planting; and (4) No_For/CO_2: no CO_2 fertilization and no harvest. Additionally, model scenarios with repeating climate (1997) (No_Clim), no vegetation dynamics (mortality, reproduction, disturbance) (No_Dyn) or neither (NO_Dyn/Clim) were tested with the 1996–2004 runs to test hypotheses on the roles of stochastic disturbance, and interannual climate variability on regional ecosystem carbon uptake.

2.5. Parameter Estimation

[30] ED requires parameters to describe many features of each plant function type (PFT) and the general ecosystem properties, as defined in Table 2. These parameters were prescribed from a combination of field observations, literature, FIA averages, model optimization tests, and sensitivity analyses. Detailed description of the parameters and equations are given by *Moorcroft et al.* [2001], *Hurtt et al.* [2002] and *Albani et al.* [2007].

[31] Choice of model PFTs was determined from remotely sensed land cover and FIA. Ecophysiological and biometric regional field observations were available for VcMax, SLA, K, β, C:N, SA:LA, and FR:LM (defined in Table 2) for many PFTs [*Bolstad et al.*, 2004; *Burrows*, 2002; *Curtis et al.*, 2002; *Kreller*, 2005; *Martin and Bolstad*, 2005; *Scheller and Mladenoff*, 2005; *Tang et al.*, 2006, 2007]. Density-independent mortality rates were taken from a ratio of FIA observed mortality rates of individual mature trees to total number of trees. Region average disturbance rates were extracted from change of forest structure (species number density and age structure) with time over recent FIA measurement cycles (1983, 1996, 2004). Growth-related mortality parameters were taken from the SORTIE model [*Deutschman et al.*, 1997]. Published literature and model defaults were used for soil turnover rates [*Schimel et al.*, 1994] and for coefficients of the power-law allometry equations [*Burrows*, 2002; *Jenkins et al.*, 2004; *Perala and Alban*, 1993; *Smith and Brand*, 1983; *Ter-Mikaelian and Korzukhin*, 1997]. A gridded soil characteristics database provided soil percolation and depth [*Miller and White*, 1998]. For PFTs where no data were available, substitutes from parameterized PFTs were taken and/or ED default parameters were applied (Table 3).

[32] Some of these parameters with no available data or those that strongly influenced model results were subject to parameter tuning with manual optimization/sensitivity tests. VcMax and β values were tuned by running ED between two FIA cycles, 1996 and 2004. FIA population density (ha^{-1}) estimates were segregated by forest type association, species, DBH, and age. FIA measurements are limited to trees greater than 2.5 cm DBH. Values from the 1996 FIA along with nominal values for other pools (soil carbon, saplings, etc.) and allometric equations were used to initialize ED in 1996. The model was then run to 2004. Model results for aboveground biomass change in trees greater than 2.5 cm DBH were compared to FIA estimates in 2004 along PFT and size gradients. VcMax values were allowed to vary by PFT until the model reasonably matched FIA

Table 2. Flux and Parameter Abbreviations and Definitions

Abbreviation	Description
GPP	gross primary production, g C m^{-2} yr^{-2}
R_a	autotrophic respiration, g C m^{-2} yr^{-2}
R_h	heterotrophic respiration, g C m^{-2} yr^{-2}
NPP	net primary production = GPP-R_a, g C m^{-2} yr^{-2}
NEE	net ecosystem exchange, g C m^{-2} yr^{-2}
ER	total ecosystem respiration = Ra+Rh, g C m^{-2} yr^{-2}
VcMax	maximum carboxylation rate at 25°C, μmol m^2 s^{-1}
SLA	specific leaf area, m^2 kg^{-1}
C:N	labile carbon to nitrogen ratio
L:N	lignin to nitrogen ratio
K	light extinction coefficient
b1	allometric equation multiplier
b2	allometric equation power coefficient
α	plant decay rate, yrs^{-1}
β	respiration rate, kg kg^{-1} yr^{-1}
SA:LA	sapwood area to leaf area, cm^2 m^{-2}
M1	SORTIE mortality intercept
M2	SORTIE mortality decay rate
DI	density-independent mortality rate
SD_MORT	seedling mortality
Global Disp.	global seed dispersal fraction
R_Fract	fraction of GPP to reproduction
FR:LM	fine root to leaf carbon mass
GR_Fract	Growth respiration fraction of NPP

Table 3. Primary ED Model PFT-Specific Parameters

		Mesic Upland				Xeric Upland				Lowland/Wetland			
Parameter	GR[a]	AS	BI	SM	HE	JP	RP	WP	RM	AL	TA	CE	BS
Leaf													
VcMax	17.5	26.2	35.8	31.6	12.2	25.4	21.0	13.0	55.9	27.1	10.2	13.9	22.1
SLA	22.5	12.1	16.9	16.6	10.2	8.2	6.8	7.4	12.7	12.0	12.2	8.3	4.5
C:N Leaf	18.7	23.6	12.5	14.3	57.9	35.8	52.0	75.4	10.7	23.0	57.2	63.2	74.6
K	2	0.5	0.511	0.511	0.625	0.4	0.4	0.5	0.511	0.5	0.5	0.3	0.3
Allometry													
Leaf - b1	0.08	0.0114	0.0085	0.0401	0.0369	0.001	0.01331	0.0404	0.0436	0.0147	0.0466	0.0111	0.0179
Leaf - b2	1	2.0261	2.003	1.695	2.030	2.903	2.122	1.817	1.540	1.828	1.725	2.303	2.383
Stem - b1	$1x10^{-5}$	0.04342	0.07335	0.15893	0.05529	0.1825	0.0775	0.0473	0.1987	0.0488	0.0762	0.0720	0.0687
Stem - b2	1.0	2.48392	2.5942	2.3321	2.3662	2.1584	2.3233	2.2815	2.2044	2.5090	2.3051	2.1453	2.2807
Height - b1	0.5	2.390	2.678	3.804	4.183	6.117	3.6337	3.5703	4.183	2.218	2.939	1.81	2.939
Height - b2	0.5	0.5296	0.6682	0.5026	0.5026	0.3579	0.5213	0.5749	0.4558	0.5335	0.5337	0.5847	0.5337
Max. DBH	0.4	75	75	120	150	50	75	150	100	50	50	80	50
DBH leaf cap	0.4	55.2	61.7	60.9	68.5	40	50.4	53	75.4	50	50	70	40
Max. Height	1.5	25	35	30	35	25	37	40	30	25	25	30	30
Plant Decay/Turnover													
Leaf α[b]	1	1	1	1	0.2	0.222	0.167	0.167	1	1	0.167	0.125	0.1
Sapwood α	0	0.4	0.4	0.4	0.4	0.05	0.1	0.1	0.4	0.4	0.4	0.4	0.4
Fine Root α	0.333	0.333	0.333	0.333	0.2	0.222	0.167	0.167	0.333	0.333	0.333	0.25	0.2
Respiration													
Sapwood β	0	0.08	0.03	0.10	0.04	0.04	0.04	0.04	0.25	0.03	0.04	0.04	0.04
Fine root β	1	0.9	0.4	0.9	0.8	0.2	0.2	0.2	0.9	0.9	0.2	0.2	0.2
SA:LA	2.564	1.335	1.335	1.335	0.360	0.360	0.360	0.363	1.335	1.335	0.360	0.360	0.360
Mortality													
M1	0.5	0.555	0.555	0.998	0.077	0.268	0.268	0.268	0.912	0.555	0.268	0.268	0.077
M2	−5	−26.7	−26.7	−47.9	−59.7	−46.7	−46.7	−46.7	−68.8	−26.7	−46.7	−46.7	−59.7
DI	0.66	0.012	0.012	0.017	0.003	0.009	0.004	0.003	0.019	0.012	0.014	0.014	0.005
SD_MORT	0.9	0.9	0.3	0.6	0.15	0.7	0.4	0.2	0.6	0.6	0.6	0.3	0.3
Reproduction													
Global Disp.	0.999	0.999	0.948	0.297	0.01	0.01	0.766	0.766	0.474	0.474	0.297	0.001	0.297
R_Fract	0.25	0.005	0.20	0.03	0.008	0.40	0.075	0.07	0.035	0.004	0.001	0.08	0.01

[a]PFT GR (Grass/Shrub) exists in each subregion with the same parameters.
[b]Leaf turnover time 1 implies deciduous phenology.

results in 2004. Over longer timescales (centuries), modeled biomass trajectory of aboveground biomass was sensitive to fractional proportion of GPP carbon allocated to reproduction (R_fract). Since no analogous field data for R_fract existed, ED was run from pre-European settlement vegetation in 1800 to 2004 and R_fract was tuned under two conditions: (1) model ecosystem structure in 2004 reflected FIA observed biomass and density in 2004 and (2) model runs without forestry and CO_2 fertilization maintained roughly a steady state ecosystem structure after initial spinup. More rigorous mathematical optimization/minimization methods were not used because of long model runtime. The method described here is admittedly simplistic and further research is warranted for parameter optimization, as discussed in section 4.3.

[33] Estimated parameters from literature, field observations, FIA, and FIA-based model tuning revealed wide variation of many parameters by PFT type and subregion (Table 3). PFT GR was used in all three subregion model runs with the same parameters as a stand-in for grass, shrubland and meadow grasses in the mesic upland, xeric upland, and lowland subregions runs, respectively. Leaf turnover time of 1 implies deciduous phenology with all leaf decay (fall) occurring during leaf drop. Leaf respiration values are not shown since they were implicit as part of the leaf-level assimilation formulation. Table 4 shows ED global model parameters and parameters that are constant across all PFTs in addition to soil decomposition parameters.

2.6. Model Evaluation

[34] Modeled monthly CO_2 fluxes were compared against the Park Falls, Wisconsin, tall tower to evaluate model performance with respect to regional flux estimation. Monthly net ecosystem exchange (NEE) measurements on the tall tower are available from 1997–2004 with the exception of 2002 due to instrument failure. Ecosystem respiration (ER) and gross primary production (GPP) were inferred from tower observations using gap-filling and flux partitioning techniques [*Cook et al.*, 2004; *Desai et al.*, 2005]. Additionally, model fluxes by forest type and age were evaluated against the ChEAS stand-scale flux tower network [*Desai et al.*, 2007] to identify potential (1) biases in model or flux tower observations, (2) undersampled ecosystems or processes that may have a large impact on

Table 4. Model Global Parameters

Parameter	Units	Value
Latitude	°N	45.95°N
Longitude	°W	90.27°W
First year	yr	1800
Final year	yr	2004
L:N leaf		10
L:N root		10
L:N structural		36
C:N stem		150
C:N root		40
C:N structural		150
C:N slow C		15
C:N passive C		15
FR:LM[a]	kg kg^{-1}	1
GR_Fract	fraction	0.533
Treefall disturbance rate	fraction	0.014
Disturbance height threshold	m	15
Disturbance age threshold	yrs	50
Canopy disturbance survival	fraction	0
Subcanopy disturbance survival	fraction	0.03
Fast soil C turnover	yrs^{-1}	12
Structural soil C turnover	yrs^{-1}	4.9
Structural lignin turnover	yrs^{-1}	4.9
Slow soil C turnover	yrs^{-1}	2
Passive soil C turnover	yrs^{-1}	0.0045
Fast soil C respiration rate	fraction	1.0
Structural soil C respiration rate	fraction	0.6
Structural lignin respiration rate	fraction	0.3
Slow soil C respiration rate	fraction	0.5
Passive soil C respiration rate	fraction	0.55

[a]Value set to 1.33 for PFT GR.

regional flux, and (3) reasons for the mismatch between tall tower regional fluxes and upscaling with the stand-scale tower network. Finally, model results were also compared to independent bottom-up regional flux estimates from the tower networks.

3. Results

3.1. Land Cover

[35] Initial land cover in 1800 for ED by PFT, age, and height was provided from public land surveys, assigned to the mesic upland (Figure 4a), xeric upland (Figure 5a), and lowland/wetland (Figure 6a) subregions and showed the primacy of hemlock and white pine forests. Given the described forcing, land use and parameters, ED-modeled land cover in 2004 for the three subregions (Figures 4d, 5d, 6d) generally reproduced the ecosystem structure observed by FIA (Figures 4c, 5c, and 6c). Also shown is ecosystem structure from FIA for 1996 (Figures 4b, 5b, and 6b), which was used in ED for the leaf-level parameter estimation short runs.

[36] When compared to FIA, the modeled ecosystem structure in 2004 was biased toward younger aged stands for mesic upland and toward older stands for xeric upland. A negative height bias is also apparent for young aspen and red pine species. The worst comparison occurred in the lowland/wetland subregion, most likely owing a combination minimal lowland sampling in FIA and poor modeling of wetland dynamics in ED. Overall, however, modeled dynamics of prior land use and anthropogenic disturbance in the region reasonably predicted current land cover in the region.

3.2. Flux Tower Evaluation

3.2.1. Tall Tower

[37] High correlations were found in comparison of the long-run ED to eddy covariance tall tower observations of monthly total NEE ($r^2 = 0.65$), GPP ($r^2 = 0.93$) and ER ($r^2 = 0.91$) over a 7-year period (Figure 7). Although the model generally performed well, capturing the seasonal cycle of NEE, GPP, and ER and including the respiration peaks at leaf drop in fall and in early spring prior to leaf out, predicted summer NEE was significantly larger than observed, due primarily to underestimation of ER. Model to observation differences in winter NEE were not significant.

[38] The model also reproduced a majority of the observed interannual variability (IAV) ($r^2 = 0.53$) in mean annual NEE, including the impact of forest tent caterpillars in 2001, a disturbance that was explicitly prescribed using the forest pathogen disturbance submodel. Growing season (June–Aug) IAV was also well modeled ($r^2 = 0.68$). Reduced late growing season NEE in 1998 was not modeled

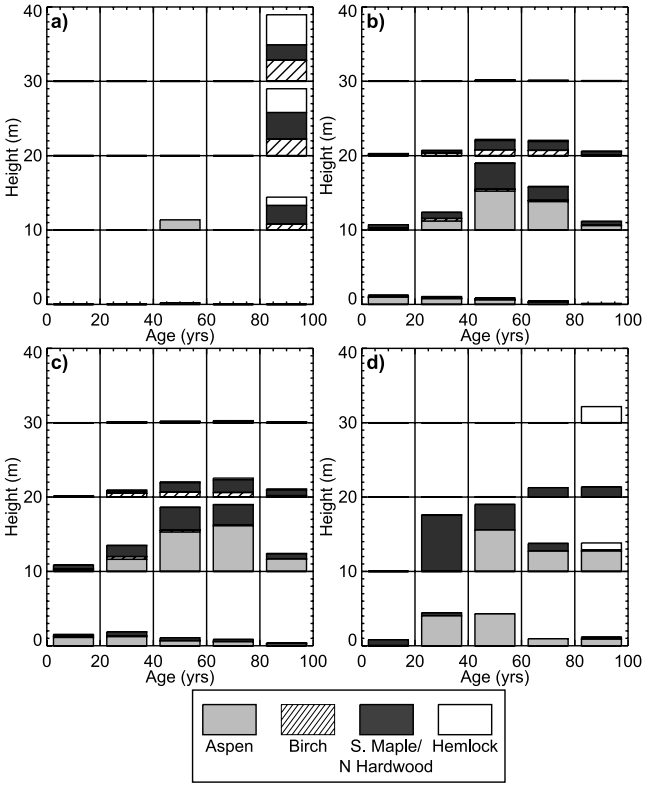

Figure 4. Mesic upland fractional PFT dominance by basal area for 20-year stand age intervals and 10-m height intervals of aspen (light gray), birch (lines), sugar maple/northern hardwoods (dark gray), and eastern hemlock (white) parameterized by land surveys in (a) 1800, (b) 1996, and (c) 2004 and predicted by long-run ED model in (d) 2004. Total bar height is scaled by maximum total grid box basal area. The model generally captures the observed forest age and height structure but with slightly more northern hardwood, less birch, and younger aspen than observed.

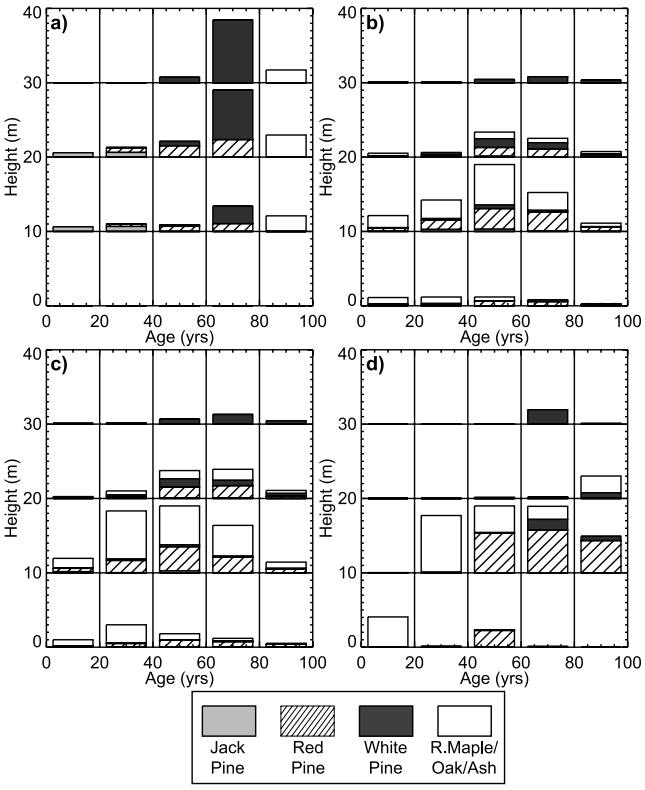

Figure 5. Same as Figure 4 but for xeric upland PFTs jack pine (light gray), red pine (lines), white pine (dark gray), and red maple/oak/ash (white). The model overestimates dominance of red pine and underestimates xeric hardwoods. The model height structure is skewed toward midheight (10–20 m) canopy members.

well. Low correlations were found in IAV of GPP ($r^2 = 0.25$) or ER ($r^2 = 0.15$), despite model ability to capture IAV in NEE. Especially notable is the low modeled ER compared to observation in 1999, in contrast to 1998. Model ER was lower than observed in 4 of 7 years.

3.2.2. Stand-Scale Towers

[39] Comparison of the model to 13 stand-scale flux sites in the region was possible since the model produced flux estimates by age and subregion. Many of these towers only ran in the growing seasons of 2002 and 2003, and as such, this period was the focus of comparison. Detailed descriptions of the 13 sites and their fluxes are given by *Desai et al.* [2007]. We segregated model ensemble gaps for those two years from June–August into 10-year patch classes and computed mean and variance statistics for each subregion. Since the Full run had very few old-growth patches, the No_For patch fluxes were used for comparison to the unlogged Sylvania old-growth site [*Desai et al.*, 2005].

[40] Correlation of model to observed growing season fluxes was high for NEE ($r^2 = 0.64$) and GPP ($r^2 = 0.59$), but low for ER ($r^2 = 0.09$) (Figure 8). The largest model-observed mismatch occurred with mature hardwood sites, where the observations showed larger NEE and GPP than modeled. Similarly, poor overall correlation to ER was mostly due to overestimation of ER in most of the mature sites except the oldest site. ER in young hardwood sites was underestimated. GPP predictions for most sites were within range of gap variance and observational error, but the mean was biased high.

3.2.3. Comparison of Scaled Flux

[41] Model results can also be compared to several other observation based bottom-up scaling of NEE, ER, and GPP. Two independent methods to scaling carbon fluxes were applied using the network of flux towers in the region. The first method (LEF*) decomposed tall tower observed flux (LEF) into ecosystem parameters using a novel ABL flux footprint model and remotely sensed landcover [*Wang et al.*, 2006]. These parameters were driven by regional meteorology and ecosystem landcover information in the 40 km radius around the tower to reaggregate the tall tower flux into a spatially conditioned regional flux [*Desai et al.*, 2007]. A second method (Towers) relied on the same land cover information, but derived parameters solely from the stand-scale towers and also incorporated stand age statistics from FIA to further segregate the land cover data [*Desai et al.*, 2007].

[42] ED model NEE was found to lie between the scaling methods (LEF*, Towers) and the tall tower (LEF) when compared over the June–August 2003 period (Table 5). The ED model had higher ER than the scaling methods, more in line with the WLEF tower observations. Model GPP was highest among the different regional flux estimates, owing to the high bias of mature GPP in the model. The largest difference in NEE between LEF and LEF* is suggestive of a

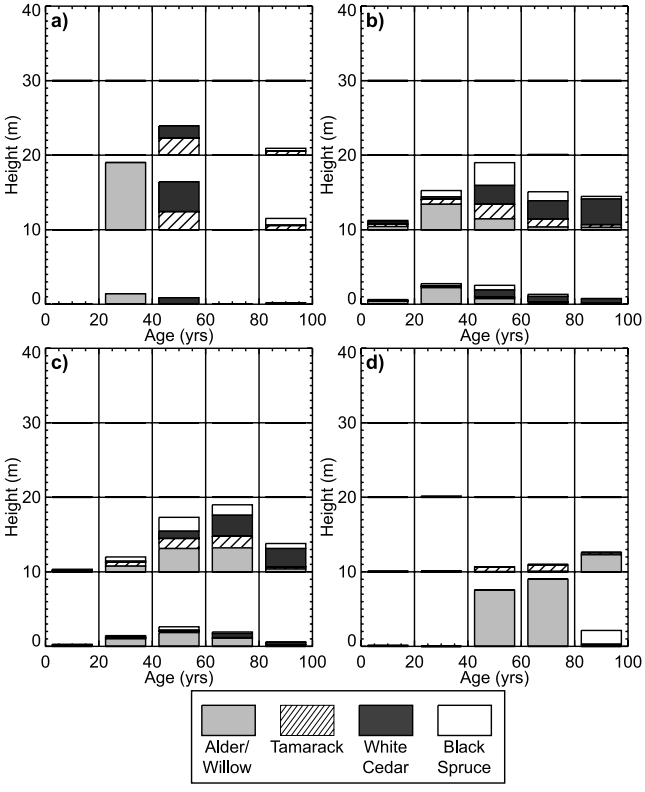

Figure 6. Same as Figure 4 but for lowland/wetland PFTs alder/willow shrub deciduous wetland (light gray), tamarack (lines), white cedar (dark gray), and black spruce (white). The model is overdominant on alder/willow at expense of other PFTs, but the accuracy of FIA based wetland cover can also be called into question.

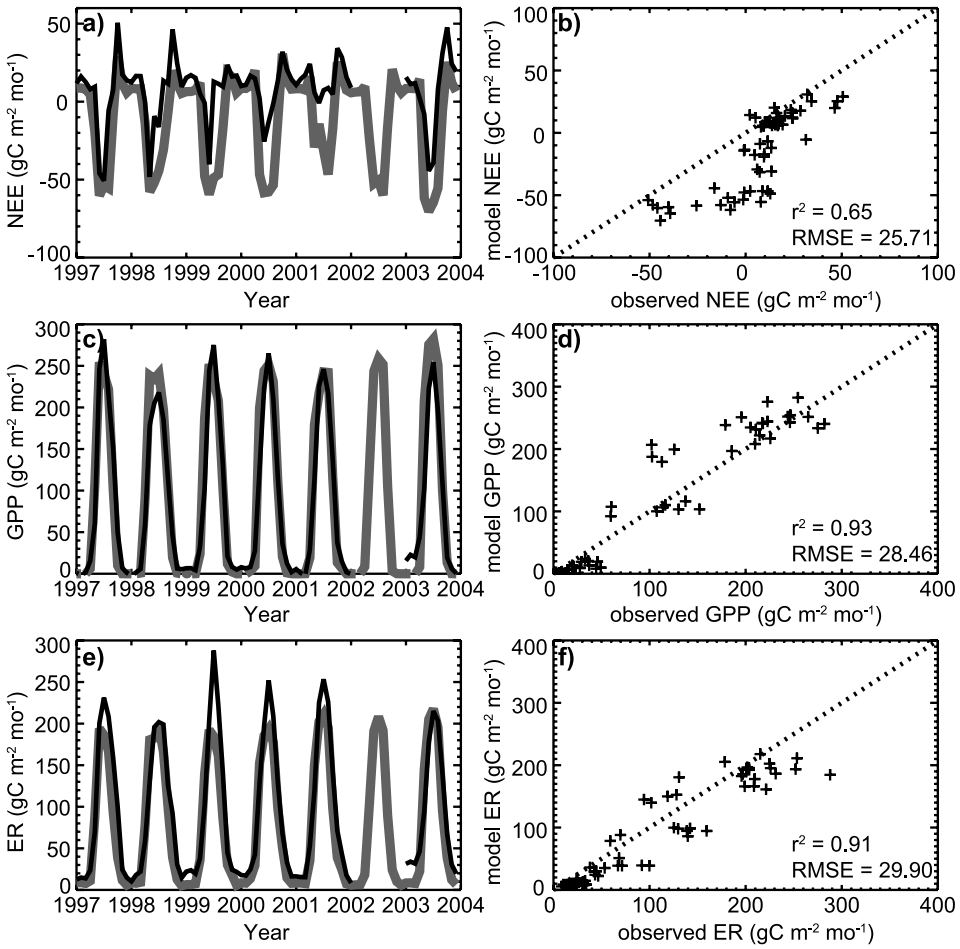

Figure 7. (left) Monthly time series and (right) 1:1 relationships as modeled by ED (gray) and observed at the tall tower (black) for (a, b) NEE, (c, d) GPP, and (e, f) ER. The model captures the observed monthly and seasonal cycle of NEE, GPP, and ER but overestimates summer peak NEE, owing to underestimation of ER. Interannual variability is modeled moderately well by the model.

flux footprint bias in the tall tower, but may also suggest lack of detailed information on forest age structure and recent disturbance when extrapolating to the entire 40-km region.

3.3. Model Scenarios

3.3.1. Forestry and Carbon Fertilization Impacts on CO_2 Flux

[43] Differences in ecosystem structure in 2004 across the model long-run scenarios reveal the long-term impact of forest harvest and rising atmospheric CO_2. Modeled forest total biomass, basal area, and total leaf area index (LAI) were 1.75–2, 1.6–1.7 and 1.5–1.7 times larger, respectively, with increased (1.4×) CO_2 than without (Table 6). Interestingly, while long-term forest harvest, planting, and land use significantly changed the mean forest stand age and ecosystem structure compared with having only natural disturbance, average stand biomass and basal area were the same with or without forest harvest; however, this is likely due to coincidence, since both forests are primarily mature canopies, but with different species mix.

[44] The effect of forestry and CO_2 on PFT dominance by relative basal area is shown in Figure 9. Although CO_2 fertilization made for a much denser forest, the composition of the modeled forest was roughly the same. The largest difference occurred between aspen and maple stands. Increasing CO_2 favored aspen growth relative to maple in the model, and even led to a change in order of dominance in the case without forestry. Without forestry, increasing CO_2 also appeared to slightly favor forested over shrub wetlands and slightly reduced hemlocks. While forestry had little effect on mean forest density in terms of biomass, LAI and basal area, the effect of harvest, and preferential planting of aspen, maple and red pine certainly affected the ecosystem structure for the upland subregions, turning a hemlock dominant forest into a mixed northern hardwood forest, providing evidence for the hypothesis of land use change determining modern ecosystem structure.

[45] Annual NEE, ER, GPP, and NPP CO_2 fluxes averaged over 1996–2004 showed that each scenario impacted these fluxes differently (Table 7). The Full run with both factors led to the largest NEE due to both the high CO_2 atmosphere and fast growing younger forests, as evidenced in the high GPP in the scenario. While ER was also highest in this scenario, owing to the impact of logging and land clearing on CWD, the increase in GPP over other scenarios was larger than the increase in ER, leading to higher NEE. The NPP model estimate from the Full run (423 gC m^{-2} yr^{-1})

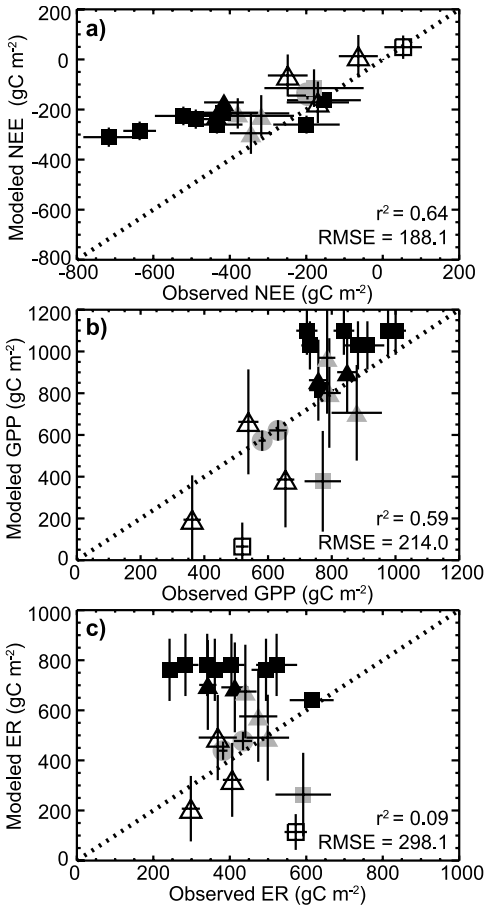

Figure 8. Comparison of independent eddy covariance observed to ED modeled summer (June–August) total (a) NEE, (b) GPP, and (c) ER for mature (black), intermediate (gray), and young (white) aged mesic upland/hardwood (square), xeric upland/conifer (triangle), and shrub wetland (circle) sites in 2002 and 2003. Error bars for model are 1 standard deviation of all flux in model patches of same age/PFT and for observations are 1 standard deviation of Monte Carlo flux variability due to gap filling missing data. The model is good at modeling NEE and GPP but significantly underestimates NEE at mature hardwood sites owing to overestimation of ER.

matched closest to a regional remote sensing scaled field observation of NPP (402–431 gC m^{-2} yr^{-1}) [*Ahl et al.*, 2005]. Thus the Full run scenario's overestimate of NEE, slight overestimate of GPP, and larger underestimate of ER compared to the tall tower and close match to biometric NPP imply that modeled heterotrophic respiration (R_h) was underestimated while autotrophic respiration (R_a) was slightly overestimated.

[46] Without CO_2 fertilization, annual NEE was much smaller and closer to the annual estimates directly observed by the tall tower. However, while annual NEE was more like the estimate from the tall tower, the improvement was a result of compensating errors: ER, GPP, and NPP were significantly lower than that estimated by the tall tower or directly scaled from field observations. Another interesting result is the appearance that CO_2 fertilization and forestry had covarying effects on GPP and ER. While forestry and land use change led to slightly smaller GPP and smaller ER in the modern CO_2 atmosphere, the same harvest, planting, and clearing rates led to slightly higher GPP and higher ER with pre-Industrial CO_2. The reason for these differences was not directly apparent from model output, though it most likely arose from the greater dominance of aspen over northern hardwood in the modern CO_2 atmosphere versus pre-Industrial (Figure 9). Overall, the results of the effects of CO_2 and land use on fluxes suggest that both CO_2 fertilization and land use had effects of similar magnitude and sign on NEE.

3.3.2. Climate Variability, Ecosystem Dynamics, and Biomass Accumulation

[47] Further investigation of the impacts of climate and ecosystem dynamics on carbon fluxes can be assessed with the short runs based on the 1996 FIA ecosystem structure. Here we test several scenarios by removing combinations of four ED model options: no forestry/land use scenario (No_For), pre-Industrial CO_2 scenario (No_CO_2), no vegetation dynamics (reproduction, mortality, disturbance) (No_Dyn), and no interannual climate variability (constant recycling of 2004 meteorology) (No_Clim). Since the short runs were based on only FIA vegetation information, the comparison focused on how these scenarios altered the 8-year annual average aboveground biomass accumulation for nonseedling trees. Recall that the short runs were used initially to adjust assimilation and growth parameters, and as such the model is a priori tuned to accurately predict biomass accumulation over the 8-year period based on the 1996 and 2004 FIA estimates of total tree biomass as seen in the "Full" scenario (Table 8).

[48] The alternate scenarios produced significantly different estimate of biomass accumulation, though the rates are all generally much smaller than total plant biomass (Table 8). With forestry, net biomass accumulation was twice as large owing both to lack of carbon export by harvest and planting of seedlings. The effect was even more dramatic when also excluding natural ecosystem dynamic processes leading to another doubling of model to observed difference in biomass accumulation. Thus, even though both germination and mortality/disturbance were not included, the overall effect was for the existing trees to grow.

[49] These effects were larger than the effects of not including interannual climate variability, which led to slightly larger estimate of biomass accumulation compared to the Full run. Pre-Industrial CO_2 corroborated the effect seen in the long runs, namely that the density of the current

Table 5. Comparison of Tall Tower Observed (LEF) to Regional Mean NEE, ER, and GPP Estimated By Tall Tower Footprint Decomposition and Reaggregation (LEF*), Multitower Synthesis Aggregation (Towers), and ED Model (Model) for Summer (June–August) 2003[a]

Method	NEE	GPP	ER
LEF	−0.80	7.10	6.30
LEF*	−2.70	6.64	3.93
Towers	−3.04	7.32	4.28
Model	−1.63	7.66	6.02

[a]Unit is μmol m^2 s^{-1}. LEF, tall tower observed; LEF*, tall tower footprint decomposition and reaggregation; Towers, multitower synthesis aggregation; Model, ED model. Summer comprises June–August.

Table 6. Model Regional Average Ecosystem State in 2004 for the Four Long-Run (1800–2004) Scenarios, Showing the Effect of Forestry and CO_2 Fertilization on Ecosystem State

Scenario	CO_2 Change	Forestry	Stand Age, years	Basal Area, m^2 ha^{-1}	Biomass, kg m^{-2}	LAI, m^2 m^{-2}
Full	yes	yes	52.1	29.5	4.7	3.6
No_CO_2[a]		yes	52.6	17.1	2.7	2.1
No_For[b]	yes		81.6	31.4	4.6	4.3
No_For/CO_2			82.1	19.6	2.3	2.8

[a]No_CO_2 denotes pre-Industrial CO_2/no CO_2 fertilization.
[b]No_For denotes no forest harvest/land use change.

forest in the model was a strong function of the available atmospheric CO_2, given the standard biogeochemical formulation used in the model. Thus, with significantly lower CO_2, biomass accumulation in the short run became negative as carbon added to the biosphere from forest biomass growth and germination of seedlings became smaller than carbon lost owing to mortality and disturbance processes.

4. Discussion

4.1. Model Performance

[50] Model CO_2 flux estimates, parameterized from field observations and land survey data, were similar to independent estimates from both tall and stand-scale eddy covariance flux towers across the region. High correlation was found for model to observed regional NEE at the monthly and annual timescale and across space. These results confirm the importance of stand age, cover type, and land use variability in determining regional CO_2 fluxes.

[51] Prediction of ecosystem structure driven by pre-European land cover, land use transition rates, natural disturbance/mortality/recruitment functions, and forest harvest/planting estimates reasonably resembled observed FIA ecosystem structure. Model ecosystem structure and/or density were markedly different from modern land cover when run without land use change or CO_2 fertilization, confirming the hypothesis of the roles of anthropogenic change in determining modern ecosystem structure and its

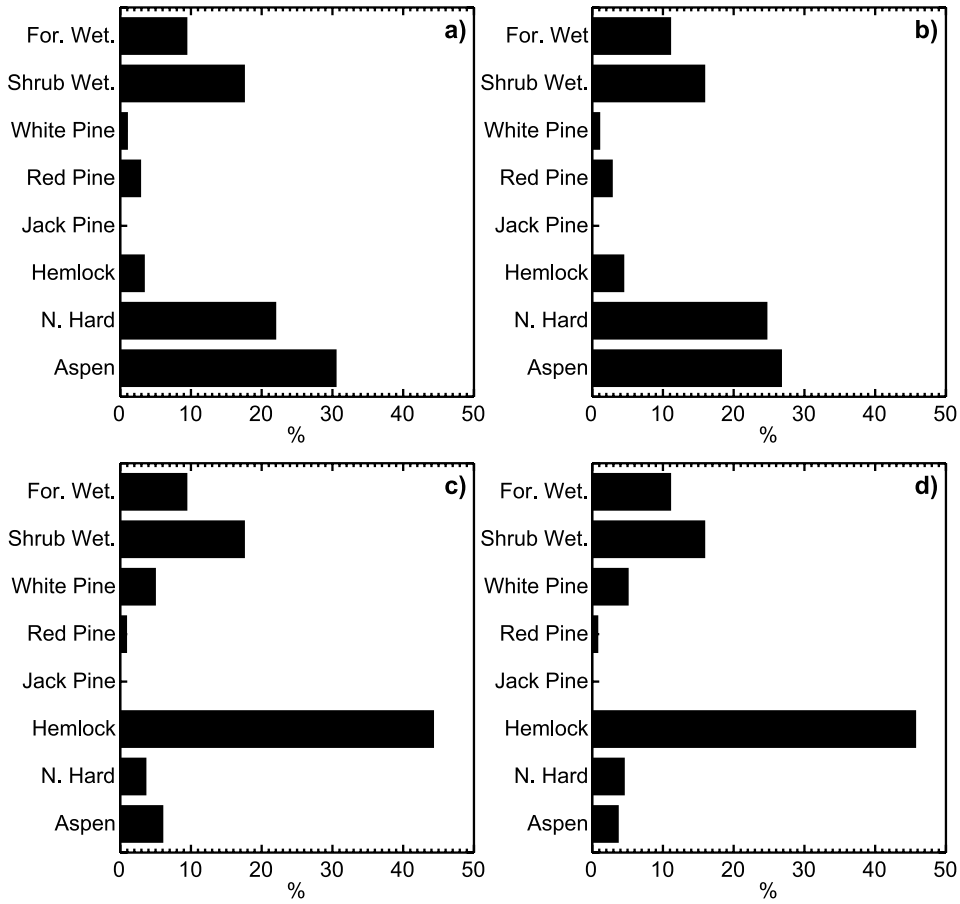

Figure 9. Model output regional land cover in 2004 by fractional basal area for the four long-run scenarios: (a) Full run, (b) pre-Industrial CO_2 (No_CO_2), (c) no forest harvest or land use change (No_For), and (d) neither CO_2 fertilization nor anthropogenic disturbance (No_For/CO_2). CO_2 fertilization had less effect on model land cover than forestry. The primary effect of CO_2 fertilization is to slightly favor growth of aspen and shrub wetlands. The primary effect of forestry is to remove the primary hemlock forest with northern hardwoods.

Table 7. Model Output Annual NEE, ER, GPP, and NPP Averaged Over 1996–2004 for the Four Long-Run Scenarios[a]

Scenario	NEE	ER	GPP	NPP
Full	−130	922	1052	426
No_CO_2[b]	−70	533	603	243
No_For[c]	−100	906	1006	402
No_For/CO_2	−50	565	615	243

[a]Unit is gC m^{-2} yr^{-1}.
[b]No_CO_2 denotes pre-Industrial CO_2/no CO_2 fertilization.
[c]No_For denotes no forest harvest/land use change.

potential for future change. However, certain biases were evident in the model. A large mismatch of model to FIA land cover occurred in the lowland/wetland subregion, as would be expected given the paucity of data on initial wetland cover, lack of model wetland/hydrology dynamics, and poor sampling of ecosystem structure in shrub and forested wetlands compared to upland forests.

[52] Despite the general corroboration of the independent flux and ecosystem structure estimates, there were several obvious discrepancies that require further scrutiny. The largest of these is the continued incongruity between the large CO_2 uptake observed in stand-scale mature hardwood towers and the much smaller uptake observed at the tall tower, due almost entirely to the larger ER observed at the tall tower. Model ER was somewhere in between, significantly higher than the mature hardwood observations, but still not as large as tall tower observations. Speculation that the source of this ER is either wetlands or recent disturbance was not entirely resolved by model results, since the model highlights high ER in both types of stands, in addition to suggesting that the mature hardwood forests have higher ER that that observed at mature hardwood eddy covariance sites in the region. In young hardwood and conifer sites, model ER was actually lower than observed from stand-scale eddy covariance towers. Recent field studies with portable eddy covariance systems in regional young aspen stands and open wetlands suggest that high ER is more likely found in the recently cut hardwood sites (N. Saliendra, personal communication, 2006).

[53] Previous studies report low tower ER estimates relative to other measurements. Upscaled field-based soil and plant chamber respiration measurements at one site [*Bolstad et al.*, 2004] were shown to be significantly larger than observed by eddy covariance, potentially owing to improper accounting of intermittent nocturnal CO_2 venting anomalies on nighttime NEE [*Cook et al.*, 2004]. Additionally, recent plot level ecosystem structure observations in forests around the tall tower suggested that the eddy covariance mature hardwood site was not representative of the region in terms of woody debris biomass and species mix.

[54] While higher correlation was found with model to observed GPP than for ER, there was still a slight high bias in model GPP at most sites. The high GPP existed despite model basal area, leaf area, and NPP being in line with regional observations. This result suggests that leaf assimilation and plant respiration parameters would benefit from additional constraints. Alternatively, there is reason to suspect that the leaf physiology submodel required additional improvements and parameter optimization. Suggestions for model improvements are discussed in more detail in section 4.3.

[55] Regardless of these disagreements, model regional growing season flux estimates were in line with the alternative tower-based parameter estimation scaling formulations. Model NEE was in between in situ tall tower observations and the regionally scaled footprint decomposition/reaggregation methods. Model regional ER was closer to the tall tower, suggesting that either the tall tower fluxes were not representative of the region or that both the stand-scale tower network and the land cover data on which the footprint decomposition reaggregation relied lacked sufficiently detailed specification of flux parameters over coverage of stand age and recent disturbance. Evidence supports both of these hypotheses.

[56] Tall tower fluxes may suffer from flux bias or error arising from spatial ecosystem footprint sampling and adverse micrometeorological conditions. Nighttime tall tower fluxes were limited to the 30-m level instead of the daytime preferred 396-m level owing to decoupling of flow between the near-surface nocturnal stable boundary layer and the residual layer [*Davis et al.*, 2003]. Nocturnal ABL depth was typically below 396 m [*Yi et al.*, 2001]. Footprint analyses supported sampling biases given that footprints at 30 m contain significantly larger representation of a grassy clearing near the tower [*Wang et al.*, 2006]. Horizontal and vertical advection may be important contributions to flux at night and are not typically measured [e.g., *Wang et al.*, 2005].

[57] Remotely sensed land cover data for the bottom-up scaling methods may be subject to errors arising from

Table 8. Annual Average Change in Aboveground Plant Biomass for Trees > 2.5 cm DBH From 1996 to 2004 as Observed by FIA or Modeled by ED Short-Run Scenarios Using 1996 FIA Land Cover as the Initial Model Cover[a]

Scenario	CO_2 Change	Forestry	Climate Variability	Vegetation Dynamics	ΔB, gC m^{-2} yr^{-1}
Observed/FIA	na	na	na	na	55.3
Full	yes	yes	yes	yes	52.3
No_For	yes		yes	yes	109.6
No_CO_2		yes	yes	yes	−61.0
No_For/CO_2			yes	yes	−12.0
No_Clim		yes		yes	72.4
No_Clim/For				yes	130.3
No_Dyn	yes		yes		251.0
No_Dyn/CO_2			yes		243.9
No_Dyn/Clim					221.0

[a]No_For, no forest harvest/land use change; No_CO_2, pre-Industrial CO_2/no CO_2 fertilization; No_Clim, no interannual variability in climate variables and CO_2; No_Dyn, no ecosystem dynamics (mortality, reproduction, natural disturbance); na, not applicable.

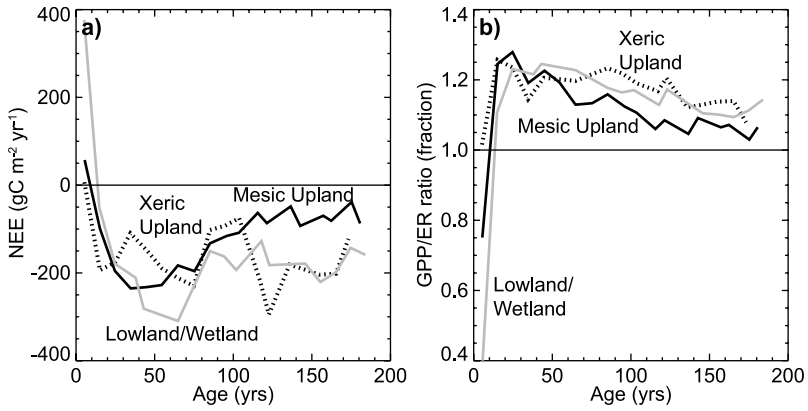

Figure 10. Modeled variation in annual (a) NEE and (b) GPP/ER with stand age for all patches over 1996–2004 in the mesic upland (black line), xeric upland (dashed line), and lowland/wetland (gray line) subregions.

spatial resolution, time since data collection, and limited differentiation of several cover types in spectroscopic space. The 30-m land cover database used by *Desai et al.* [2007] and *Wang et al.* [2006] was based on data collected in 1992 and thus is missing disturbance events in the last decade. Additionally, separation of forest from shrub wetland and hardwood from aspen cover classes has been shown to have lower accuracy than other cover type classifications in the data set. FIA data used in the multitower aggregation was limited to forest cover only, with limited coverage in wetlands.

4.2. Impact of Disturbance, Land Use, and CO_2 on Regional Flux

[58] Model scenarios revealed that natural disturbance processes, land use, atmospheric CO_2 concentration, and interannual climate variability cannot be neglected for ecosystem-atmosphere CO_2 flux modeling. The short-run scenarios revealed that model ecosystem dynamics and land use affected average biomass accumulation even on relatively short (decadal) timescales. The traditional assumption by ecosystem models that CO_2 fluxes on the short timescale are influenced exclusively by interannual climate variability and atmospheric CO_2 concentration, which may be true for models at the stand scale, does not capture the observed flux spatial and temporal variability at regional and larger scales. Prediction of flux on decadal or greater timescales requires consideration of both climate variability and ecosystem dynamics.

[59] Over the long timescale, the ED model had a strong response to CO_2 fertilization, similar to many ecosystem models that use the standard Farquhar leaf-level photosynthesis equations [*El Maayar et al.*, 2006]. Whether ecosystems actually respond so vigorously (e.g., a near doubling in biomass) to a almost 40% increase in CO_2 over 150 years is unknown, and is a general area of disagreement in the modeling community. Not all models produce such a strong response [e.g., *Thornton et al.*, 2002]. Other factors such as nitrogen limitation, leaf physiological changes, changes in biological competition, water-use limitation and temperature mediated changes in respiration could all counter balance the enhanced growth expected by higher CO_2. The covariance of twentieth century forest regrowth and increasing CO_2 further complicates the picture for modeling CO_2 fertilization. Here, since the model was tuned to reproduce observed forest structure in the modern CO_2 atmosphere, there may some reason to doubt both the timing of modeled forest recovery in the twentieth century post-harvest and also the validity of results in the No_CO_2 scenarios. More research is definitely warranted.

[60] A salient feature of ED is the ability to examine multiple stand ages simultaneously within a particular grid cell at a particular time. The effect of stand age on NEE can be directly investigated with the ED model given the model's age, size and PFT structured formulation (Figure 10a). Here NEE was segregated by 10-year patch age intervals over the 1996–2004 timeframe. Since the Full run did not contain patches of significant size over age 80 (to improve computation speed, the model removed gaps and reapportioned its carbon if they fell below an area threshold), patches for old sites were taken from the no forestry run. The model revealed NEE that was positive (source to atmosphere) in young sites, especially lowland wetlands, rapidly became negative (sink to biosphere) within 10–20 years, peaked around 40–70 years, and declined with age afterward. This decline was stronger in the mesic upland subregion than for wetland or xeric upland subregions.

[61] GPP:ER ratios (Figure 10b) in all subregions peaked early and slowly declined with age. ED also calculated that old sites remained small carbon sinks due to the effects of subcanopy growth, regular mortality and increasing CO_2, in agreement with modern observations of NEE in old-growth forests [e.g., *Desai et al.*, 2005], but in contrast to traditional assumptions of carbon neutrality in old growth. Even though the GPP:ER ratio declined with age, the model GPP and ER both increased with age, but ER increased faster than GPP, as the canopy cover closed while stems continued to grow and CWD quantity increased.

[62] While both young and old stand age sites had high ER, the source of the ER varied (Figure 11). Recent disturbance ER was primarily driven by heterotrophic respiration (R_h) from coarse woody debris (CWD) and the existing soil organic matter pool. As forests grow, autotrophic respiration (R_a) becomes the dominant source of respiration, according to the model. Though the modeled

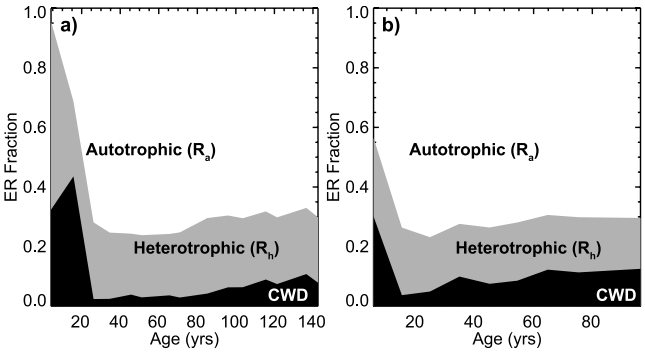

Figure 11. Modeled variation in autotrophic (R_a), heterotrophic (R_h), and coarse woody debris (CWD) respiration fraction of total ER with stand age over all patches from 1996–2004 (a) without (scenario No_For) anthropogenic disturbance and (b) with (scenario Full).

R_a/R_h ratio in mature and old sites was higher than typical theoretical assumptions (0.5), it was relatively similar to chamber-based respiration observations in the region [*Martin and Bolstad*, 2005; *Tang et al.*, 2007].

[63] Moreover, the partition of ER into components varied on presence or absence of forestry. Without forestry (Figure 11a), most ER after disturbance was R_h, due to the impact of respiration on CWD. However, the export of living and salvaged trees and the planting of fast growing commercial species in the Full run changed the mix toward majority R_a (Figure 11b), with overall ER higher. The different species mix and dynamics then changed the long term buildup of CWD with age. Modeled CWD respiration in old unlogged sites was as high as young sites, though a smaller overall fraction since R_a was much larger. This scenario was less the case in sites with active management. Thus flux observations in existing old-growth sites may not necessarily be reflective of future NEE in the region as harvest rates decline and existing managed forest ages.

4.3. Sources of Error and Potential Model Improvements

[64] Though this adaptation of ED for use in the upper Midwest provided promising results, model results would benefit from including additional observations, refining parameter estimates, and improving model processes. Continued advances in observation platforms, parameter estimation techniques and ecological theories will improve our ability to model ecosystems; however, there are also existing observations and techniques that deserve consideration. We consider a few here.

[65] In terms of additional observations, greater information on forest and wetland structure, change in structure with time and direct observation of ecosystem parameters that can be used by ED with little modification are warranted. Given that ED is an age and height structured model, the use of spatial forest structure information (e.g., from lidar) has been shown to improve ED initialization [*Hurtt et al.*, 2004]. Additionally, existing spatial information on leaf area [*Ahl et al.*, 2004] and aggregated component NPP [*Burrows*, 2002] in the immediate area around the tall tower deserve consideration for inclusion. Time series of remote sensing images can also be used to obtain recent disturbance rates [e.g., *Masek and Collatz*, 2006; *Zheng et al.*, 2004]. Assimilation and transpiration parameters would also benefit from incorporation of existing observations of transpiration from sap flux [*Mackay et al.*, 2002; *Tang et al.*, 2006], especially given the high leaf-level transpiration in the model compared to observations.

[66] Parameter tuning and estimation techniques have been rapidly advancing in the last decade. *Raupach et al.* [2005] argue that both parameter estimates and their known error covariances are required for proper assimilation of observational data into model parameters. The complexity and computational demands of ED limits full utilization of the most involved optimization methods, but there is value in simplifying model structure to the core parameters of interest and using optimization techniques such as Markov Chain Monte Carlo, as has been done for the tall tower observations [*Ricciuto et al.*, 2007]. Formal sensitivity analyses and multiple model comparison can also help reveal key parameters that require the closest tuning [e.g., *Cramer et al.*, 2001].

[67] ED was recently coupled to a regional atmospheric model (RAMS) for parameter optimization in a single forest stand in the northeast U.S. (Harvard Forest) using eddy covariance data and regional forest structure (D. Medvigy et al., Mechanistic scaling of ecosystem function and dynamics in space and time: The Ecosystem Demography model version 2, submitted to *Global Change Biology*, 2007). Results from that study indicated that adjustments to several ED model default parameters values resulted in substantial improvements in the ability of the model to predict seasonal and long-term patterns of CO_2 uptake. While some of these new parameters were adopted in this study (for example, increasing the fraction of GPP to growth respiration from a default of 0.333 to 0.533), a similar optimization method could be employed with the ChEAS data set. In this study, the ED model was found to be especially sensitive to a few parameters, namely VcMax, R_fract and disturbance/mortality rates. Lack of observations of these parameters in some or all PFTs required a hybrid tuning approach, which was admittedly simplistic.

[68] Many model processes could be investigated for improvement. Some of these include inclusion of CO_2 downregulation in high atmospheric CO_2 [*El Maayar et al.*, 2006], 3-D light scattering and attenuation in complex canopies, more realistic seedling recruitment scenarios [*Matthes and Larson*, 2006; *Mohan et al.*, 2004], complex seed dispersal functions [*Scheller and Mladenoff*, 2005], changes in SLA with age/height [*Niinemets*, 2006], herbivory effects on sapling mortality [*Kneeshaw et al.*, 2006], forest edge effects and spatial interaction in patchy landscapes [*Euskirchen et al.*, 2001], public/private ownership effects on forest harvest and structure [*Crow et al.*, 1999], and forest product lifecycle analysis and harvest economic optimization strategies as a replacement for the probabilistic forest harvest functions currently in ED [*Scheller and Mladenoff*, 2005; *White et al.*, 2005]. Some of these improvements are currently in consideration for the next iteration of ED and related models [e.g., *Albani et al.*, 2007; O. Soong and P. R. Moorcroft, manuscript in preparation, 2007]. Of course, caution is always warranted when refining

models given the typical tradeoff between model complexity and number of free parameters.

5. Conclusion

[69] This study found the following.

[70] 1. The Ecosystem Demography (ED) model, a statistical, dynamic ecosystem model, when initialized with pre-European settlement land cover, parameterized and tuned with field observations, and forced with historical climate and land use data, was able to reasonably reproduce the statistical properties of species, age, and height ecosystem structure in the 40-km radius around the northern Wisconsin very tall tower. Worse comparison was found with wetland/lowland forest owing to lack of cover information, parameters and wetland dynamics and biogeochemistry in the model.

[71] 2. Without twentieth century atmospheric CO_2 increase or land use change/forestry, modeled ecosystem structure was significantly different than observed. The effect of CO_2 increase was to almost double forest density, while forestry and land use change almost halved the average forest stand age and significantly changed the species composition. Minor interaction effects between the two forcings on ecosystem structure were also observed.

[72] 3. Model NEE, GPP and ER were highly correlated to tall eddy covariance flux tower observations on both monthly and annual timescales over the 8-year measurement record. Similar to other models, modeled growing season NEE had a stronger sink than the tall tower due almost entirely to lower ER in the model. However, growing season model CO_2 uptake was smaller than two independent regional bottom-up estimates based on eddy covariance parameter optimization and land cover aggregation, due to higher ER modeled in poorly sampled recently disturbed forests and wetlands.

[73] 4. Model results were able to explain a majority of the variance in NEE and GPP across the region and ER in young and intermediate stands as observed by a network of stand-scale eddy covariance flux towers, confirming the hypothesis that stand age is the key factor explaining regional flux variability. The notable exception are mature hardwood sites, where the model predicted slightly higher GPP and much larger ER, the latter more in line with chamber flux observations. Model results support recent observations that suggest the mature hardwood sites in the network are not necessarily reflective of the region. The model had a high GPP bias at most sites, suggesting that additional processes controlling plant CO_2 assimilation are needed in ED.

[74] 5. Young stand age sites were sources of CO_2 to the atmosphere due to high CO_2 respiration in disturbed biomass CWD. Export of forest biomass by forestry reduced the impact of respiration. Old-growth sites continued to be carbon sinks due to overstory growth continuing to exceed mortality rates of subcanopy individuals.

[75] 6. As a dynamic ecosystem model, ED was especially sensitive to reproduction, recruitment, mortality, and disturbance parameters in addition to CO_2 assimilation parameters. Additional spatial observations, model improvements and advanced data assimilation methods are required to further constrain model fluxes.

[76] While the model was not able to fully solve the question of the observed tall tower net annual CO_2 source in the regional landscape, it did provide strong evidence on the role of stand age, disturbance, and wetlands on ecosystem structure and fluxes at the regional scale. Nondynamic ecosystem models that use constant ecosystem structure/properties and/or constant atmospheric CO_2 across time will significantly misestimate current CO_2 fluxes in managed, patchy landscapes. Given that managed landscapes are representative of most of the terrestrial biosphere, prediction of future biosphere response to climate change and increasing CO_2 will require specification of land management and land use change and exploration of the potential for multiway feedbacks between climate, land management, and CO_2 fluxes.

Appendix A: ED Model Overview

[77] The ED model tracks the time evolution of fractional area of ensemble-average patches of different ages since disturbance and number density of ensemble-average plant cohorts of different height and species in each patch. Patches are tracked in time by fractional grid cell coverage, p (m^2 m^{-2}), and are labeled with age since disturbance, a (years), and disturbance type i: primary (natural disturbance), secondary (anthropogenic disturbance) and agricultural (cleared land). Patches also track the mass (kg) of five coarse woody debris pools (CWD), four soil organic carbon pools (fast, slow, structural, passive), one structural lignin pool, three soil nitrogen pools (mineralized, fast, passive), and two soil water pools (0–5 cm, >5 cm). Cohorts are tracked by number density (individuals m^{-2}) and labeled with height, h (m), living biomass, z_a (kg), structural biomass, z_s (kg), and a plant function type parameter vector, x (PFT).

[78] In the partial differential equation (PDE) form, the core ED equation for cohort number density is [*Albani et al.*, 2007; *Hurtt et al.*, 2002]

$$\frac{\partial}{\partial t} n_i(\bar{z},\bar{x},a,t) = \left\{ \begin{array}{ll} \dfrac{\partial}{\partial z_s}[g_s(\bar{z},\bar{x},\bar{r},t) n_i(\bar{z},\bar{x},a,t)] & (i) \\ \dfrac{\partial}{\partial z_a}[g_a(\bar{z},\bar{x},\bar{r},t) n_i(\bar{z},\bar{x},a,t)] & (ii) \\ -\mu(\bar{z},\bar{x},\bar{r},t) n_i(\bar{z},\bar{x},a,t) & (iii) \\ \dfrac{\partial}{\partial a} n_i(\bar{z},\bar{x},a,t) & (iv) \end{array} \right\} \quad \text{(A1)}$$

where subscript i is disturbance type, z is an ensemble-average vector of z_a and z_s, and x is the PFT with PFT-specific parameters. The frame of reference coordinates for n are time, t (years), a, z_a, and z_s. Functions g_s, g_a and μ describe structural biomass growth, living (active) biomass growth, and mortality, respectively. These functions depend on r, the resource vector, which contains the ensemble-average plant environment conditioned on age and size and includes light, meteorology, water, and nutrient data. Mortality functions are based on prescribed rates for density-independent mortality and the SORTIE model [*Deutschman et al.*, 1997] for density-dependent mortality, which is a function of average tree diameter increment

over the past 2.5 years. Mortality parameters are listed in Tables 3 and 4.

[79] Equation (A1) describes the time evolution of ensemble-average cohort number density of size z, type x, and age a for (i) change in structural biomass, (ii) change in living biomass, (iii) mortality, and (iv) aging. The primary boundary condition for Equation (A1) is recruitment of new seedlings of size z_0. Recruitment is based on allocation of fraction of net primary production (NPP) to reproduction (R_fract), fractional dispersal of "seeds" to other patches and germination of new cohorts of prescribed initial size z_0, and number density R_fract/z_0 (Table 3).

[80] The PDE describing patch age distribution evolution [*Albani et al.*, 2007; *Hurtt et al.*, 2002] is

$$\frac{\partial}{\partial t}p_i(a,t) = \left\{ \begin{array}{ll} -\frac{\partial}{\partial a}p_i(a,t) & (i) \\ -\lambda_i(a,t)p_i(a,t) & (ii) \\ -\sum_j \lambda_{j,i}(a,t)p_i(a,t) & (iii) \end{array} \right\}$$
$$\int_0^\infty \sum_i p_i(a,t) = 1 \qquad \text{(A2)}$$
$$p_i(0,t) = \int_0^\infty \lambda_i(a,t)p_i(a,t) + \sum_j \lambda_{i,j}(a,t)p_j(a,t)$$

where i and j subscripts are disturbance types, λ_i is a disturbance rate, and $\lambda_{j,i}$ is a land-use transition rate from type i to type j. Equation (A2) describes the time evolution of fractional cover of patches of age a and disturbance type i as a function of (i) aging, (ii) disturbance, and (iii) land-use change. The bottom two equations in equation (A2) are the boundary conditions, which constrains patches to cover the entire grid cell and describes the formation of recently disturbed patches. Equation (A2) also leads to an additional boundary condition for Equation (A1), which is the state of cohorts after a disturbance event. These can be specified as natural disturbance events that lead to mortality of canopy cohorts above specified age and height thresholds, harvest events that lead to removal or thinning of cohorts above minimum diameter at breast height (DBH), and clearing events that lead to creation of agricultural patches that do not age and contain no cohorts. Additional PDEs of similar form are also given for the below ground soil carbon (four pools: fast, structural, slow and passive), soil lignin, soil nitrogen (three pools: fast, mineralized and passive), and soil water (two pools: 0–5 cm and >5 cm). Tables 3 and 4 list related parameters.

[81] Growth functions are based on the well-established leaf-level biogeochemical models of *Farquhar et al.* [1980], *Farquhar and Sharkey* [1982], *Ball et al.* [1987], *Collatz et al.* [1991], and *Leuning* [1995] and similar to those used in the well-known models IBIS [*Foley et al.*, 1996] and HYBRID [*Friend et al.*, 1997]. Leaf-level assimilation and evaporation are found on an hourly time step for a range of light levels and maximum carboxylation rates and integrated to a monthly timescale. To solve the dynamic PDEs, the plant available resources (light, water, nutrients) are also conditioned on age and canopy position. As in the work of *Moorcroft et al.* [2001], carbon allocation functions maintain plant allometric relationships unless plants are in negative carbon balance. Allometric equations (with parameters listed in Table 3) for leaf carbon biomass, aboveground stem carbon biomass, and tree height were all of the power-law form:

$$b_1 DBH^{b_2}. \qquad \text{(A3)}$$

[82] By rewriting PDEs into a patch age and cohort size moving frame of reference, the equations can be reformed as loosely coupled stiff ordinary differential equations (ODEs), which can then be solved with standard adaptive time step (days-month) ODE integration techniques. By nature of the model framework and assumption of sufficiently large number of gaps, ED is essentially scale-independent up to the spatial scale at which significant variation in abiotic factors (climate, soil, topography) are prescribed.

Appendix B: Snow Hydrology

[83] To better capture the impact of winter season precipitation on regional carbon dynamics, a snow hydrology module was added to ED. Monthly precipitation is divided into rain water ($RAIN_{in}$, mm mo^{-1}) and snow water equivalent (S_{in}, mm mo^{-1}) on the basis of the fraction of days per month with minimum temperature below 0°C. This method provided a reasonable approximation of observed snow accumulation in the region. Snowpack (S_{pack}, mm) and snow liquid (SL, mm) were parameterized with a simple integrative accumulation, melting and evaporation formulation based on the snow water balance formulation used in the CENTURY model version 5 [*Hilinski*, 2005],

$$S_{pack}(t) = S_{pack}(t-1) + S_{in}(t)$$
$$S_{melt}(t) = \left\{ \begin{array}{ll} 40(T+8) & T > -8 \\ 0 & T \le -8 \\ S_{pack}(t) & 40(T+8) \ge S_{pack}(t) \end{array} \right\}$$
$$S_{pack}(t) = S_{pack}(t) - S_{melt}(t); SL(t) = SL(t-1) + S_{melt}(t)$$
$$E_{avail}(t) = \min\left\{ \begin{array}{l} 1 \\ \frac{S_{pack}(t) + S_{liq}(t)}{0.87PET(t)} \end{array} \right\} \qquad \text{(B1)}$$
$$S_{evap}(t) = E_{avail}(t)S_{pack}(t); SL_{evap}(t) = E_{avail}(t)SL(t)$$
$$S_{pack}(t) = (1 - E_{avail}(t))S_{pack}(t); SL(t) = (1 - E_{avail}(t))SL(t)$$
$$SL_{soil}(t) = \max\left\{ \begin{array}{l} SL(t) - 0.05S \\ 0 \end{array} \right\}$$
$$SL(t) = SL(t) - SL_{soil}(t)$$

where t is time (months), T is air temperature (°C), S_{melt} is snow melt (mm mo^{-1}), and E_{avail} is an evaporation function (%). PET is potential evapotranspiration (mm mo^{-1}), a function of air temperature based on work by *Thornthwaite*

[1948]. The algorithm is run from the beginning to end of the snow year, September–June. Snow liquid is added to the soil (SL_{soil}) so as to keep SL no more than 5% of S_{pack}.

Appendix C: Canopy Precipitation and Evaporation

[84] Growing season ED model runs revealed soil volumetric water content higher than observed for the given precipitation. To improve model physics, a canopy filtration and canopy/soil evaporation schema were added on the basis of the CENTURY model version 5 [*Hilinski*, 2005]. This filtration model is

$$
\begin{aligned}
&C_{\mathrm{int}}(t) = RAIN_{in}(t)(0.82LAI)\\
&PET_w(t) = PET(t) - S_{evap} - SL_{evap}\\
&C_{evap}(t) = \min\left\{ \begin{matrix} 0.2C_{\mathrm{int}}(t) \\ 0.65PET_w(t) \end{matrix} \right\} \qquad \text{(C1)}\\
&Soil_{evap}(t) = \min\left\{ \begin{matrix} \left(C_{in}(t) - C_{evap}(t)\right)0.4e^{-2L-4B} \\ 0.4PET_w(t) \end{matrix} \right\} if\ S_{pack} > 0\ else\ 0\\
&W_{in}(t) = C_{\mathrm{int}}(t) + SL_{soil} - C_{evap}(t) - Soil_{evap}(t)
\end{aligned}
$$

where C_{int} is canopy intercepted water (mm mo^{-1}), $RAIN_{in}$ is incoming precipitation (mm mo^{-1}), LAI is canopy total leaf area index (m^2 m^{-2}), PET_w is PET reduced for snow evaporation (mm mo^{-1}), C_{evap} is canopy evaporation (mm mo^{-1}), $Soil_{evap}$ is bare ground evaporation corrected for canopy and litter (mm mo^{-1}), L is litter biomass (kg), B is plant aboveground biomass (kg), and W_{in} is net addition of water to the soil (mm mo^{-1}). Runoff is not included in this model. To account for topographic pooling of water in lowlands, it is assumed that water percolating from the bottom of upland soils is added to lowland soil moisture. The simplest way to account for this topographic runoff is to increase net precipitation for wetlands by a multiplicative factor, which in this case was found to be 2.

Appendix D: Soil Temperature and Decay

[85] Given model output results that showed greater than observed uptake during periods of soil temperature <0°C, the leaf assimilation model was modified to force stomatal closure during periods of soil temperature below 0°C. This effect was important to include for early and late growing season photosynthesis. Also, the current ED model did not include patch level soil temperature variability. However, observations showed moderate soil temperature variability across sites as a function of incoming solar radiation at the soil surface. Therefore a simple modification was made to incorporate this effect. Soil temperature variability across several sites with different maximum LAI and also across time was found to roughly follow:

$$T_{s,LAI} = T_s + \left(LAI\left(\frac{T_s - T_a}{16}\right)\right) + \left(\frac{T_a - T_s}{2}\right), \qquad \text{(D1)}$$

where $T_{s,LAI}$ is the canopy cover adjusted soil temperature, T_s is soil temperature (°C), T_a is air temperature (°C), and LAI is leaf area index (m^2 m^{-2}). This new soil temperature was used for calculation in the moisture and temperature respiration limitation function of ED [*Albani et al.*, 2007]. Patch level soil moisture variability as a function of evapotranspiration is already included in ED. The functional forms of the decomposition temperature/moisture limitation function are

$$
\begin{aligned}
T_d &= \left(\frac{T_{\max} - T_{s,LAI}}{T_{\max} - T_{opt}}\right)^{T_{shr}} e^{\frac{T_{shr}}{T_{shl}}\left(1 - \left(\frac{T_{\max} - T_{s,LAI}}{T_{\max} - T_{opt}}\right)^{T_{shl}}\right)}\\
W_d &= \left(\frac{\theta - B}{A - B}\right)^{D\frac{B-A}{A-C}}\left(\frac{\theta - C}{A - C}\right)^{D} \qquad \text{(D2)}\\
A &= T_d W_d
\end{aligned}
$$

where $T_{s,LAI}$ is canopy-cover modified soil temperature, θ is soil water mass fraction (kg kg^{-1}), T_d and W_d are the temperature and moisture limitation factors (0–1), and A is the combined effect of the two. Constants are T_{max} = 45°C, T_{opt} = 35°C, T_{shr} = 0.2, T_{shl} = 2.63, A = 0.6, B = 1.27, C = 0.0012, and D = 2.84.

[86] Fast, structural, slow, and passive turnover times and respiration rates are noted in Table 4 and are subject to the water and temperature limitation factor, A. Structural soil organic matter decomposition is additionally limited by a factor based on the ratio of structural soil carbon to lignin content. Fast and structural carbon are limited by nitrogen immobilization and mineralization as described by *Moorcroft et al.* [2001].

Appendix E: PFT Parameters

[87] Field observations allowed for modification of two ED parameters that in the current model are considered the same for all PFTs. The first, shortwave light extinction coefficient, is assumed to be 0.5 in the Beer's Law relationship. Data from *Kreller* [2005] and the SORTIE model [*Deutschman et al.*, 1997] provide PFT-specific light extinction coefficients (Table 3). *Kreller* [2005] showed that scaling estimates of GPP from leaf to the stand scale was highly sensitive to choice of this coefficient. Field data also allowed for PFT specific sapwood area to leaf area (SA:LA) ratios [*Tang et al.*, 2006; E. Carey, unpublished data, 2003]. In ED, sapwood biomass is based on a plant "pipe" model and found as the product of SA:LA (m^2 m^{-2}), specific leaf area (m^2 kg^{-1}), leaf biomass (kg), wood carbon density (kg m^{-3}), and tree height (m). Field data and literature estimates were used to find PFT-specific SA:LA ratios instead of a constant value for all species (Table 3). Though the net effect of this was small, the PFT-varying SA:LA did slightly modify carbon allocation in the active biomass pool between leaf, sapwood and fine root.

Appendix F: Leaf Phenology and Pests

[88] The phenology model in ED is based on (1) climatology-based growing degree day threshold computed as a function of number of days with temperature below 0°C prior to leaf out and (2) daylight and soil temperature thresholds for leaf off. During leaf off, 50% of existing leaf biomass is added to litter and the other 50% is put in a "virtual" leaf pool that does not photosynthesize or respire.

The virtual leaf pool is added back to the plant during leaf out.

[89] To incorporate phenology observations derived from above and below canopy shortwave radiation observations, ED was modified to allow for prescribed phenology after a certain date. The phenology model was also modified to simulate the effect of a forest tent caterpillar outbreak in 2001, which had a significant impact on observed carbon flux. During May and June of 2001, 50% of existing leaf biomass from deciduous species was ''eaten'' and sent to the litter pool to decay. Reflush of leaves then occurs automatically owing to the ED model ''off-allometry'' carbon allocation routines.

Appendix G: Reproduction and Seedling Germination

[90] The original ED model allocated reproductive carbon from NPP year round and germinated this carbon in the same month with the same sapling mortality rate for all PFTs. Given the long cold season in the upper midwest and the high sensitivity of the model to reproduction and carbon fraction allocation, modifying the reproduction/germination module was needed to more realistically reflect the plant reproductive lifecycle. Reproduction allocation fraction of NPP was allowed to vary by PFT (Table 3). Allocation was limited to trees above a minimum reproductive height and then only from June to October, which is when most plants produce fruit. These ''seeds'' were dropped and added to a seedbank from August to November. A PFT specific fractional seedbank decay rate was then applied. Decayed seed biomass was added to the fast litter pool. Germination occurred 1 month after leaf flush for deciduous species, when soil temperature were between 7°–18°C for evergreen species, and when temperature was greater than 20°C or when a fire occurred for fire-adapted cones, such as jack pine. For species with delayed germination, only a fraction of the seedbank germinated and the remaining stayed in the seedbank for potential germination in the next season, with seedbank decay rates applied.

Appendix H: Harvest and Tree Planting

[91] Forest harvest in ED is treated as simple fractional disturbances for primary and secondary type patches. Harvest survival rates were slightly modified to reflect regional practices. For a harvest, 3% of tree less than 3 cm DBH survive and 0% of trees with diameter greater than that. Since the model region is small, 90% of harvested above ground stem is exported from the grid cell to decay elsewhere. The remaining stem (e.g., stump), belowground material, and leaves are added to the litter pool and decay on site. Harvested patches are planted with one of two PFTs per submodel. For mesic upland, a conditioned random selection planted aspen 2 out of 3 times and sugar maple the rest of the time. For xeric upland, red pine was planted 2 out of 3 times and red maple/ash/oak the other times. Plantation stocking rates were set to be consistent with FIA observations.

[92] **Acknowledgments.** The authors wish to acknowledge the help of numerous field crew, technicians, engineers, and students involved in installation, maintenance, troubleshooting, and data collection at all the sites. Model support was provided by Dan Lippsitt, Marco Albani, and David Medvigy of Harvard University. We appreciate the valuable discussions with Steve Wofsy, Harvard University, and George Hurtt, University of New Hampshire, and the comments from anonymous reviewers. We wish to thank the land owners for allowing access to field locations, including the cooperation of the U.S. Department of Agriculture (USDA) U.S. Forest Service (USFS), Chequamegon-Nicolet National Forest, USDA USFS Ottawa National Forest, the Wisconsin Educational Communications Board, and Roger Strand, chief engineer for WLEF-TV. We also acknowledge the support of field stations such as the University of Wisconsin Kemp Natural Resources Station for housing personnel, storing equipment, and providing lab access. These sites and this analysis were funded in part with support from the U.S. National Science Foundation, grant 0129405, U.S. Department of Energy (DOE), Office of Science (BER), Terrestrial Carbon Processes program, grant DE-FG02-00ER63023, U.S. DOE BER Midwestern Regional Center of the National Institute for Global Environmental Change under Cooperative Agreement DE-FC03-90ER61010, National Aeronautics and Space Administration (NASA) Science Mission Directorate, National Oceanic and Atmospheric Administration (NOAA) Climate Monitoring and Diagnostics Lab (CMDL), USDA USFS Northern Global Change Research Program, and the USDA USFS North Central Research Station.

References

Adams, D. M., R. W. Haynes, and A. J. Daigneault (2006), Estimated timber harvest by U. S. region and ownership, 1950–2002, *Gen. Tech. Rep. PNW-GTR-659*, 64 pp., Pac. Northwest Res. Stn., For. Serv., U.S. Dep. of Agric., Portland, Oreg.

Ahl, D. E., S. T. Gower, D. S. Mackay, S. N. Burrows, J. M. Norman, and G. R. Diak (2004), Heterogeneity of light use efficiency in a northern Wisconsin forest: Implications for modeling net primary production with remote sensing, *Remote Sens. Environ.*, *93*, 168–178.

Ahl, D. E., S. T. Gower, D. S. Mackay, S. N. Burrows, J. M. Norman, and G. R. Diak (2005), The effects of aggregated land cover data on estimating NPP in northern Wisconsin, *Remote Sens. Environ.*, *97*, 1–14.

Albani, M., G. C. Hurtt, and P. R. Moorcroft (2007), The contributions of land-use change, CO_2 fertilization and climate variability to the carbon sink in the eastern United States, *Global Change Biol.*, *12*, 2370–2390, doi:10.1111/j.1365-2486.2006.01254.x.

Baker, I., A. S. Denning, N. Hanan, L. Prihodko, M. Uliasz, P. L. Vidale, K. Davis, and P. Bakwin (2003), Simulated and observed fluxes of sensible and latent heat and CO_2 at the WLEF-TV tower using SiB2.5, *Global Change Biol.*, *9*, 1262–1277.

Bakwin, P. S., P. P. Tans, C. L. Zhao, W. Ussler, and E. Quesnell (1995), Measurements of carbon-dioxide on a very tall tower, *Tellus, Ser. B*, *47*, 535–549.

Ball, J. T., I. E. Woodrow, and J. A. Berry, (1987), A model predicting stomatal conductance and its contribution to the control of photosynthesis under different environmental conditions, in *Proceedings of the International Congress on Photosynthesis: Progress in Photosynthesis Research*, edited by I. Biggins, pp. 221–224, Martinus Nijhoff, Zoetermeer, Netherlands.

Birdsey, R. A., and G. M. Lewis (2003), Current and historical trends in use, management, and disturbance of U.S. forestlands, in *The Potential of U.S. Forest Soils to Sequester Carbon and Mitigate the Greenhouse Effect*, edited by J. M. Kimble et al., pp. 15–33, CRC Press, Boca Raton, Fla.

Bolstad, P. V., K. J. Davis, J. M. Martin, B. D. Cook, and W. Wang (2004), Component and whole-system respiration fluxes in northern deciduous forests, *Tree Physiol.*, *24*, 493–504.

Braswell, B. H., W. J. Sacks, E. Linder, and D. S. Schimel (2005), Estimating diurnal to annual ecosystem parameters by synthesis of a carbon flux model with eddy covariance net ecosystem exchange observations, *Global Change Biol.*, *11*(2), 335, doi:10.1111/j.1365-2486.2005.00897.x.

Bristow, K. L., and G. S. Campbell (1984), On the relationship between incoming solar radiation and daily maximum and minimum temperature, *Agric. For. Meteorol.*, *31*, 159–166.

Burrows, S. N. (2002), Geostatistical estimation of leaf area index and net primary production of five North American biomes, Ph.D. thesis, 198 pp., Univ. of Wis.-Madison, Madison.

Caspersen, J. P., S. W. Pacala, J. C. Jenkins, G. C. Hurtt, P. R. Moorcroft, and R. A. Birdsey (2000), Contributions of land-use history to carbon accumulation in US forests, *Science*, *290*, 1148–1151.

Collatz, G. J., J. T. Ball, C. Grivet, and J. A. Berry (1991), Physiological and environmental regulation of stomatal conductance, photosynthesis and transpiration: A model that includes a laminar boundary layer, *Agric. For. Meteorol.*, *53*, 107–136.

Cook, B. D., et al. (2004), Carbon exchange and venting anomalies in an upland deciduous forest in northern Wisconsin, USA, *Agric. For. Meteorol.*, *126*(3–4), 271–295, doi:10.1016/j.agrformet.2004.06.008.

Cramer, W., et al. (2001), Global response of terrestrial ecosystem structure and function to CO_2 and climate change: Results from six dynamic global vegetation models, *Global Change Biol.*, *7*, 357–373.

Crow, T. R., G. E. Host, and D. J. Mladenoff (1999), Ownership and ecosystem as sources of spatial heterogeneity in a forested landscape, Wisconsin, USA, *Landscape Ecol.*, *14*, 449–463.

Curtis, P. S., P. J. Hanson, P. Bolstad, C. Barford, J. C. Randolph, H. P. Schmid, and K. B. Wilson (2002), Biometric and eddy-covariance based estimates of annual carbon storage in five eastern North American deciduous forests, *Agric. For. Meteorol.*, *113*, 3–19.

Davis, K. J., P. S. Bakwin, C. Yi, B. W. Berger, C. Zhao, R. M. Teclaw, and J. G. Isebrands (2003), The annual cycles of CO_2 and H_2O exchange over a northern mixed forest as observed from a very tall tower, *Global Change Biol.*, *9*, 1278–1293.

Desai, A. R., P. Bolstad, B. D. Cook, K. J. Davis, and E. V. Carey (2005), Comparing net ecosystem exchange of carbon dioxide between an old-growth and mature forest in the upper midwest, USA, *Agric. For. Meteorol.*, *128*(1–2), 33–55, doi:10.1016/j.agrformet.2004.09.005.

Desai, A. R., et al. (2007), Influence of vegetation and seasonal forcing on carbon dioxide fluxes across the Upper Midwest, USA: Implications for regional scaling, *Agric. For. Meteorol.*, in press.

Deutschman, D. H., S. A. Levin, C. Devine, and L. A. Buttel (1997), Scaling from trees to forests: Analysis of a complex simulation model, *Science*, *277*, 1688.

El Maayar, M., N. Ramankutty, and C. J. Kucharik (2006), Modeling global and regional net primary production under elevated atmospheric CO_2: On a potential source of uncertainty, *Earth Interact.*, *10*, 1–20.

Euskirchen, E. S., J. Q. Chen, and R. C. Bi (2001), Effects of edges on plant communities in a managed landscape in northern Wisconsin, *For. Ecol. Manage.*, *148*(1–3), 93–108.

Farquhar, G. D., and T. D. Sharkey (1982), Stomatal conductance and photosynthesis, *Annu. Rev. Plant Physiol.*, *33*, 317–345.

Farquhar, G. D., S. von Caemmerer, and J. A. Berry (1980), A biochemical model of photosynthetic CO_2 assimilation in leaves of C_3 species, *Planta*, *149*, 78–90.

Foley, J. A., I. C. Prentice, N. Ramankutty, S. Levis, D. Pollard, S. Sitch, and A. Haxeltine (1996), An integrated biosphere model of land surface processes, terrestrial carbon balance, and vegetation dynamics, *Global Biogeochem. Cycles*, *10*, 603–628.

Frelich, L. E. (1995), Old forest in the lake states today and before European settlement, *Nat. Areas J.*, *15*, 157–167.

Frelich, L. E., and P. B. Reich (1995), Neighborhood effects, disturbance, and succession in forests of the western Great-Lakes region, *Ecoscience*, *2*, 148–158.

Friend, A. D., A. K. Stevens, R. G. Knox, and M. G. R. Cannell (1997), A process-based terrestrial biosphere model of ecosystem dynamics, *Ecol. Modell.*, *95*, 249–287.

Hanson, P. J., et al. (2004), Oak forest carbon and water simulations: Model intercomparisons and evaluations against independent data, *Ecol. Monogr.*, *74*(3), 443–489.

Heinsch, F. A., et al. (2006), Evaluation of remote sensing based terrestrial productivity from MODIS using regional tower eddy flux network observations, *IEEE Trans. Geosci. Remote Sens.*, *44*(7), 1908–1925, doi:10.1109/TGRS.2005.853936.

Hilinski, T. (2005), *CENTURY User's Guide and Reference*, Natl. Resour. Ecol. Lab., Fort Collins, Colo. (Available at http://www.nrel.colostate.edu/projects/century5/reference/index.htm)

Hughes, P. Y., E. H. Mason, T. R. Karl, and W. A. Brower (1992), *United States Historical Climatology Network Daily Temperature and Precipitation Data*, 140 pp., Carbon Dioxide Inf. Anal. Cent., Oak Ridge Natl. Lab., Oak Ridge, Tenn.

Hurtt, G. C., S. W. Pacala, P. R. Moorcroft, J. Caspersen, E. Shevliakova, R. A. Houghton, and B. Moore (2002), Projecting the future of the US carbon sink, *Proc. Natl. Acad. Sci. U. S. A.*, *99*, 1389–1394.

Hurtt, G. C., R. Dubayah, J. Drake, P. R. Moorcroft, S. W. Pacala, J. B. Blair, and M. G. Fearon (2004), Beyond potential vegetation: combining lidar data and a height-structured model for carbon studies, *Ecol. Appl.*, *14*, 873–883.

Jenkins, J. C., R. A. Birdsey, and Y. Pan (2001), Biomass and NPP estimation for the mid-Atlantic region (USA) using plot-level forest inventory data, *Ecol. Appl.*, *11*, 1174–1193.

Jenkins, J. C., D. C. Chojnacky, L. S. Heath, and R. A. Birdsey (2004), Comprehensive database of diameter-based biomass regressions for North American tree species, *Gen. Tech. Rep. NE-319*, 45 pp., Northeast. Res. Stn., For. Serv., U.S. Dep. of Agric., Newtown Square, Pa.

Keeling, C. D., and T. P. Whorf (2005), Atmospheric CO_2 records from sites in the SIO air sampling network, in *Trends: A Compendium of Data on Global Change*, Carbon Dioxide Inf. Anal. Cent., Oak Ridge Natl. Lab., Oak Ridge, Tenn.

Kimball, J. S., S. W. Running, and R. Nemani (1997), An improved method for estimating surface humidity from daily minimum temperature, *Agric. For. Meteorol.*, *85*, 87–98.

Kneeshaw, D. D., R. K. Kobe, K. D. Coates, and C. Messier (2006), Sapling size influences shade tolerance ranking among southern boreal tree species, *J. Ecol.*, *94*(2), 471–480, doi:10.1111/j.1365-2745.2005.01070.x.

Knorr, W., and J. Kattge (2005), Inversion of terrestrial ecosystem model parameter values against eddy covariance measurements by Monte Carlo sampling, *Global Change Biol.*, *11*, 1333–1351.

Kreller, L. J. (2005), Gross primary production (GPP) of an old-growth forest in Michigan's upper peninsula: Variation in leaf physiology and simple scaling, M.S. thesis, 87 pp., Univ. of Minn., St. Paul.

Law, B. E., D. Turner, J. Campbell, O. J. Sun, S. Van Tuyl, W. D. Ritts, and W. B. Cohen (2004), Disturbance and climate effects on carbon stocks and fluxes across western Oregon USA, *Global Change Biol.*, *10*, 1429–1444.

Leuning, R. (1995), A critical appraisal of a combined stomatal-photosynthesis model for C3 plants, *Plant Cell Environ.*, *18*, 339–355.

MacKay, D. S., D. E. Ahl, B. E. Ewers, S. T. Gower, S. N. Burrows, S. Samanta, and K. J. Davis (2002), Effects of aggregated classifications of forest composition on estimates of evapotranspiration in a northern Wisconsin forest, *Global Change Biol.*, *8*, 1253–1265.

Martin, J. G., and P. V. Bolstad (2005), Annual soil respiration in broad-leaf forests of northern Wisconsin: Influence of moisture and site biological, chemical, and physical characteristics, *Biogeochemistry*, *73*, 149–182.

Masek, J. G., and G. J. Collatz (2006), Estimating forest carbon fluxes in a disturbed southeastern landscape: Integration of remote sensing, forest inventory, and biogeochemical modeling, *J. Geophys. Res.*, *111*, G01006, doi:10.1029/2005JG000062.

Matthes, U., and L. W. Larson (2006), Microsite and climatic controls of tree population dynamics: An 18-year study on cliffs, *J. Ecol.*, *94*(2), 402–414, doi:10.1111/j.1365-2745.2005.01083.x.

Miller, D. A., and R. A. White (1998), A conterminous United States multilayer soil characteristics dataset for regional climate and hydrology modeling, *Earth Interact.*, *2*, 1–26.

Mohan, J. E., J. S. Clark, and W. H. Schlesinger (2004), Genetic variation in germination, growth, and survivorship of red maple in response to subambient through elevated atmospheric CO_2, *Global Change Biol.*, *10*, 233–247.

Moorcroft, P. R. (2003), Recent advances in ecosystem-atmosphere interactions: An ecological perspective, *Proc. R. Soc., Ser. B*, *270*, 1215–1227.

Moorcroft, P. R., G. C. Hurtt, and S. W. Pacala (2001), A method for scaling vegetation dynamics: The ecosystem demography model (ED), *Ecol. Monogr.*, *71*, 557–585.

Niinemets, Ü. (2006), The controversy over traits conferring shade-tolerance in trees: Ontogenetic changes revisited, *J. Ecol.*, *94*(2), 464–470, doi:10.1111/j.1365-2745.2006.01093.x.

Pacala, S. W., and D. H. Deutschman (1997), Details that matter: The spatial distribution of individual trees maintains forest ecosystem function, *Oikos*, *74*, 357–365.

Pacala, S. W., C. D. Canham, J. Saponara, J. A. Silander, R. K. Kobe, and E. Ribbens (1996), Forest models defined by field measurements: Estimation, error analysis and dynamics, *Ecol. Monogr.*, *66*, 1–43.

Pacala, S. W., et al. (2001), Consistent land- and atmosphere-based US carbon sink estimates, *Science*, *292*, 2316–2320.

Perala, D. A., and D. H. Alban (1993), Allometric biomass estimators for aspen-dominated ecosystems in the upper Great Lakes, *Res. Pap. NC-314*, 42 pp., North Central For. Exper. Stn., For. Serv., U.S. Dep. of Agric., St. Paul, Minn.

Ramankutty, N., and J. A. Foley (1999), Estimating historical changes in land cover: North American croplands from 1850 to 1992, *Global Ecol. Biogeogr.*, *8*, 381–396.

Raupach, M. R., P. J. Rayner, D. J. Barrett, R. S. DeFries, M. Heimann, D. S. Ojima, S. Quegan, and C. C. Schmullius (2005), Model-data synthesis in terrestrial carbon observation: Methods, data requirements and data uncertainty specifications, *Global Change Biol.*, *11*, 378–397.

Ricciuto, D. M., M. P. Butler, K. J. Davis, B. D. Cook, P. S. Bakwin, A. E. Andrews, and R. M. Teclaw (2007), A Bayesian synthesis inversion of simple respiration and GEP models with eddy covariance data in a northern Wisconsin forest: Determining the causes of interannual variability, *Agric. For. Meteorol.*, in press.

Robertson, A., et al. (2001), Hypothesized climate forcing time series for the last 500 years, *J. Geophys. Res.*, *106*(D14), 14,783–14,803.

Sacks, W. J., D. S. Schimel, R. K. Monson, and B. H. Braswell (2006), Model-data synthesis of diurnal and seasonal CO_2 fluxes at Niwot Ridge, Colorado, *Global Change Biol.*, *12*, 240–259.

Scheller, R. M., and D. J. Mladenoff (2005), A spatially interactive simulation of climate change, harvesting, wind, and tree species migration and projected changes to forest composition and biomass in northern Wisconsin, *USA, Global Change Biol.*, *11*(2), 231–307, doi:10.1111/j.1365-2486.2005.00906.x.

Schimel, D. S., B. H. Braswell, E. A. Holland, R. McKeown, D. S. Ojima, T. H. Painter, W. J. Parton, and A. R. Townsend (1994), Climatic, edaphic, and biotic controls over storage and turnover of carbon in soils, *Global Biogeochem. Cycles*, *8*, 279–293.

Schimel, D. S., et al. (1997), Continental scale variability in ecosystem processes: Models, data and the role of disturbance, *Ecol. Monogr.*, *67*, 251–271.

Schimel, D. S., et al. (2001), Recent patterns and mechanisms of carbon exchange by terrestrial ecosystems, *Nature*, *414*, 169–172.

Schulte, L. A., D. J. Mladenoff, and E. V. Nordheim (2002), Quantitative classification of a historic northern Wisconsin (USA) landscape: Mapping forests at regional scales, *Can. J. For. Res.*, *32*, 1616–1638.

Smith, J. E., L. S. Heath, and P. B. Woodbury (2004), How to estimate forest carbon for large areas from inventory data, *J. For.*, *102*, 25–31.

Smith, W. B., and G. J. Brand (1983), Allometric biomass equations for 98 species of herbs, shrubs, and small trees, *Res. Note NC-299*, North Central For. Exper. Stn., For. Serv., U.S. Dep. of Agric., St. Paul, Minn.

Tang, J., P. V. Bolstad, B. E. Ewers, A. R. Desai, K. J. Davis, and E. V. Carey (2006), Sap-flux-upscaled canopy transpiration, stomatal conductance and water use efficiency in an old-growth forest in the Great Lakes region of United States, *J. Geophys. Res.*, *111*, G02009, doi:10.1029/2005JG000083.

Tang, J., P. V. Bolstad, A. R. Desai, J. M. Martin, B. D. Cook, K. J. Davis, and E. V. Carey (2007), Ecosystem respiration and its components in an old-growth forest in the Great Lakes region of the United States, *Agric. For. Meteorol.*, in press.

Ter-Mikaelian, M. T., and M. D. Korzukhin (1997), Biomass equations for sixty-five North American tree species, *For. Ecol. Manage.*, *97*, 1–24.

Thornthwaite, C. W. (1948), An approach toward a rational classification of climate, *Geogr. Rev.*, *38*, 55–94.

Thornton, P. E., et al. (2002), Modeling and measuring the effects of disturbance history and climate on carbon and water budgets in evergreen needleleaf forests, *Agric. For. Meteorol.*, *113*, 185–222.

Wang, W., K. J. Davis, B. D. Cook, P. S. Bakwin, C. Yi, M. P. Butler, and D. M. Ricciuto (2005), Surface layer CO_2 budget and advective contributions to measurements of net ecosystem–atmosphere exchange of CO_2, *Agric. For. Meteorol.*, *135*(1–4), 202–214, doi:10.1016/j.agrformet.2005.11.018.

Wang, W., K. J. Davis, B. D. Cook, D. M. Ricciuto, and M. P. Butler (2006), Decomposing CO_2 fluxes measured over a mixed ecosystem at a tall tower and extending to a region: A case study, *J. Geophys. Res.*, *111*, G02005, doi:10.1029/2005JG000093.

White, M. K., S. T. Gower, and D. E. Ahl (2005), Life cycle inventories of roundwood production in northern Wisconsin: Inputs into an industrial forest carbon budget, *For. Ecol. Manage.*, *219*, 13–28.

Woodall, C. W., P. D. Miles, and J. S. Vissage (2005), Determining maximum stand density index in mixed species for strategic-scale stocking assessments, *For. Ecol. Manage.*, *216*, 367–377.

Yi, C., K. J. Davis, B. W. Berger, and P. S. Bakwin (2001), Long-term observations of the dynamics of the continental planetary boundary layer, *J. Atmos. Sci.*, *58*, 1288–1299.

Zheng, D. L., J. Rademacher, J. Q. Chen, T. Crow, M. Bresee, J. le Moine, and S. R. Ryu (2004), Estimating aboveground biomass using Landsat 7 ETM+ data across a managed landscape in northern Wisconsin, USA, *Remote Sens. Environ.*, *93*, 402–411.

P. V. Bolstad, Department of Forest Resources, University of Minnesota, 1530 Cleveland Avenue North, Saint Paul, MN 55108, USA.

K. J. Davis, Department of Meteorology, Pennsylvania State University, 503 Walker Building, University Park, PA 16802, USA.

A. R. Desai, Institute for Integrative and Multidisciplinary Earth Studies (TIIMES), National Center for Atmospheric Research, P.O. Box 3000, Boulder, CO 80307, USA. (adesai@ucar.edu)

P. R. Moorcroft, Department of Organismic and Evolutionary Biology, Harvard University, HUH, 22 Divinity Avenue, Cambridge, MA 02138, USA.